

Time-dependent thermal convection, mantle differentiation and continental-crust growth

Uwe Walzer and Roland Hendel

Institut für Geowissenschaften, Friedrich-Schiller-Universität, 07749 Jena, Germany. E-mail: walzer@geo.uni-jena.de

Accepted 1997 March 10. Received 1997 February 17; in original form 1996 August 1

SUMMARY

The thermal evolution of the Earth is controlled by radioactive elements whose heat production rate decays with time and whose spatial distribution depends on chemical segregation processes.

We present a 2-D and finite-difference Boussinesq convection model with temperature-dependent viscosity and time- and space-dependent radioactive heat sources. We used Newtonian rheology, boxes of aspect ratio 3, and heating from within. Starting from the geochemical results of Hofmann (1988), it is assumed that the radioactive heat sources of the mantle were initially distributed homogeneously. In a number of calculations, however, higher starting abundances of radioactive sources were assumed in the upper mantle. For the present geological situation, this also results in a depleted upper mantle. It was assumed that, if the viscosity falls below a certain critical value, chemical segregation will take place. In this way, model continental crust develops, leaving behind areas of a depleted mantle. We obtained the heat source, flow line, temperature, viscosity and heat-flow distribution as a function of time with realistic values, especially for the present time. The present viscosity of the upper mantle is approximately at the standard value obtained for postglacial uplift modelling; the deeper-mantle viscosity is considerably higher. The time dependence of the computed mean of the kinetic energy of mantle convection bears a resemblance to that of the magmatic and orogenic activity of the Earth. We assumed that the 670 km discontinuity cannot be penetrated by the flow.

Key words: continental evolution, mantle convection.

1 INTRODUCTION

It has already been found (Gastil 1960) that igneous and metamorphic mineral dates are not randomly distributed on the continents, but are arranged in belts, depending on the age of the prevailing orogeneses. When these global dates are plotted over the time axis, they do not exhibit a random distribution. Similarly, the periods of large-scale transgressions and formation of strata-bound metal-sulphide ore deposits showed a relatively regular pattern of Wilson-like cycles, at least in the Phanerozoic (Tittley 1993). At least in the Phanerozoic, the worldwide transgressions occurred at times during which the reversals of the polarity of the geomagnetic dipole are rare (Walzer 1981). This observation is an indication of the presence of significant mass and heat transport in the *whole* mantle. Although this is generally accepted today, irrespective of the question whether whole-mantle convection or layered convection prevails, geophysicists at that time held the view that convection would have to be limited to the upper mantle.

There are several methods for determining the addition rate to the continental crust. Whereas the oceanic crust and the remaining oceanic lithosphere participate directly in mantle convection, the continental crust is relatively stable. If we proceed from the assumption of a very low or vanishing recycling rate for the continental crust, we also come to the conclusion, from a geochemical point of view, that, prior to 3.9 Ga, virtually all of the continental crust was formed through segregation from the mantle material and from the subducting oceanic slabs (Warren 1989). The latter constitute, after all, part of the mantle circulation. The growth considered in this approach is always the *net* growth of the continental crust in time and not the accretion of other already-existing continental parts to a continent. If, however, a relatively large subduction of continental material (e.g. $0.6 \text{ km}^3 \text{ a}^{-1}$), as compared to a worldwide continental-crust addition rate (e.g. $1.65 \text{ km}^3 \text{ a}^{-1}$), is assumed, one naturally will arrive at a more recent mean age of the continental crust (Reymer & Schubert 1984). The significance of the different continental crustal growth curves will be discussed in another paper. However, the radiogenic

age determinations performed on granites, granodiorites, gneisses etc., provide information on the age of the regional metamorphism and anatexis. We want to compare them with the periods of strong thermal mantle convection calculated in our models.

Spohn & Breuer (1993) have already developed a model of mantle differentiation by the production of continental crust. While their model is based on parametrized equations, the feed-back processes causing, in our view, the irregular variations in the magmatic and orogenic activity of the Earth can be better represented by a complete fluid-dynamic model. Our model shows some (although only slight) similarity to Ogawa's (1993) coupled magmatism-mantle-convection system.

We observe *another* type of segregation from the mantle material in the eruptions of voluminous iron- and magnesium-rich large igneous provinces (Coffin & Eldholm 1994). These ocean-basin flood basalts, continental flood basalts, volcanic passive margins, etc., are not formed together with the normal mid-oceanic-ridge basalt and obviously show an episodic distribution in time; the distribution over the time axis, however, is different from the case of the net growth rate of the continents and different again from the case of regional metamorphism and the melting of existing continental material.

Christensen & Hofmann (1994) have simulated the formation of the basaltic oceanic crust, its subduction and the hypothetical formation of the D'' layer in 2-D numerical convection models, with the D'' layer acting as a source of plumes. The negative buoyancy of the basalt or eclogite was represented by tracers. In our model considered below, the tracers have a different task. Moreover, we are essentially interested in the formation and episodic transformation of the *continent* and are basically modelling the thermal evolution associated therewith.

Models have already been developed for various aspects of the time-dependent thermal convection. Hansen & Ebel (1988) found out that it is not just the Rayleigh number, but also the aspect ratio and the initial conditions that have a decisive bearing on whether we observe steady-state or time-dependent convection. Christensen & Yuen (1989) also studied the time-dependence of bottom-heated, 2-D convection. They found that at higher Rayleigh numbers the flows in non-Newtonian rheology showed greater temporal and spatial fluctuations than in Newtonian rheology. Weinstein, Olson & Yuen (1989) also found that the time-dependent behaviour of constant-viscosity convection in large-aspect-ratio configurations starts earlier than in boxes with an aspect ratio $a = 1$. Constant-viscosity convection for a compressible mantle and internal heating becomes time-dependent at very small Rayleigh numbers (Machetel & Yuen 1989). Using non-Newtonian temperature- and pressure-dependent rheologies of olivine, Schmeling & Marquart (1993) and Schmeling & Bussod (1996) showed that the time dependence of upper-mantle convection is characterized by vigorous convective peaks associated with rising plumes or sinking blobs, followed by rather quiescent periods of sluggish convection.

The present study is based on the findings that there exist isotopically distinct source reservoirs in the mantle, and that the concentration of radiogenic heat sources in the continental upper crust is significantly higher than that of any other reservoir. As is well-known, the former follows from the isotope geochemistry of basalts, while direct evidence exists for the latter finding. We proceed from the assumption that there was

neither a continental nor an oceanic crust, but a primordial silicate mantle (*cf.* Section 2.4) with homogeneously distributed radiogenic heat sources in the initial stage of the Earth's evolution. The task we are now faced with is to find out the underlying causes of the formation of the heat-source anomalies during the evolution of the Earth, and to determine the feed-back of the inhomogeneous source distribution on the time dependence of thermal convection. In our study, a temperature- and pressure-dependent Newtonian viscosity is assumed. The influence of the 670 km phase boundary is discussed in Section 2.3.

2 THEORY AND DEVELOPMENT OF THE GEOPHYSICAL MODELS

2.1 Fluid mechanics

The full set of fluid dynamic equations describing the problem of variable viscosity convection with variable heat sources is given, discussed and simplified in Appendix A. We apply the Oberbeck-Boussinesq approximation, which was introduced by Oberbeck (1879, 1880). It has often been attributed only to Boussinesq (1903). The essence of the approximation is first that the density depends only linearly and weakly on temperature and is independent of pressure, and second that the thermal expansion coefficient, the thermal conductivity, the specific heat at constant pressure, the gravitational acceleration and the shear viscosity are constant. Regarding the shear viscosity, we deviate from this complete form of the Oberbeck-Boussinesq approximation. Furthermore, we assume 2-D flow at infinite Prandtl number. The heat equation then reduces to

$$\frac{\partial T}{\partial t} + \frac{\partial \psi}{\partial z} \frac{\partial T}{\partial x} - \frac{\partial \psi}{\partial x} \frac{\partial T}{\partial z} = \frac{\partial^2 T}{\partial x^2} + \frac{\partial^2 T}{\partial z^2} + H(x, z, t), \quad (2.1)$$

where x and z are the horizontal and vertical components of the non-dimensional location vector, t is the non-dimensional time, T is the non-dimensional temperature and ψ is the non-dimensional stream function. Eq. (2.1) follows essentially from the energy conservation equation, the (non-dimensional) specific heat production H being calculated from

$$H = \sum_{v=1}^4 a_{\mu v} a_{i v} H_{0v} \exp(-t/\tau_v). \quad (2.2)$$

The subscripts $v=1, 2, 3, 4$ refer to the radionuclides ^{40}K , ^{232}Th , ^{235}U and ^{238}U , respectively. $a_{\mu v} = a_{\mu v}(x, z, t)$ is the abundance of the element. In order to discriminate it from the aspect ratio a , we have introduced an index μ , because $a_{\mu v}$ is a non-dimensional *mass* ratio. $a_{\mu v}$ is a function of location and time. Later on, we introduce markers in order to characterize the chemical reservoirs. The abundance of the element of the radionuclide v in a pure reservoir is $a_{\mu v}^{(\zeta)}$ where the superscript (ζ) denotes the pure chemical reservoir. Tracers of different reservoirs can be in an (x, z) mesh. The abundance $a_{\mu v}(x, z, t)$ is the average of the $a_{\mu v}^{(\zeta)}$ of all tracers that are situated in a mesh around the point (x, z) at time t . $a_{i v}$ is the (also non-dimensional) isotopic abundance factor, where i stands for isotopic factor. Its values are given in Table 1. τ_v is the decay time or the $1/e$ life and H_{0v} the specific isotopic heat production 4.55×10^9 a ago (at the beginning of the evolution of the Earth). H_{0v} and τ_v and t must be made non-dimensional. H_{0v} and τ_v are also listed in Table 1.

Since we allow for chemical differentiation (or segregation)

Table 1. Data on major heat-producing isotopes.

isotope	⁴⁰ K	²³² Th	²³⁵ Th	²³⁸ U
ν	1	2	3	4
τ_i [Ma]	2015.3	20212.2	1015.4	6446.2
$H_{\nu i}$ [Wkg ⁻¹]	0.272×10^{-3}	0.0330×10^{-3}	47.89×10^{-3}	0.1905×10^{-3}
$a_{\nu i}$	0.000119	1	0.0071	0.9928

under certain conditions, the $a_{\nu i}$ are not just carried along with the flow, but undergo certain changes, as geochemical experience has shown. This will be discussed below in greater detail. For 2-D incompressible flow the equation of balance of momentum (A1) yields

$$4 \frac{\partial^2}{\partial x \partial z} \left(\eta \frac{\partial^2 \psi}{\partial x \partial z} \right) + \left(\frac{\partial^2}{\partial z^2} - \frac{\partial^2}{\partial x^2} \right) \times \left[\eta \left(\frac{\partial^2 \psi}{\partial z^2} - \frac{\partial^2 \psi}{\partial x^2} \right) \right] = Ra \frac{\partial T}{\partial x}, \quad (2.3)$$

where the Rayleigh number Ra serves only as a scaling quantity:

$$Ra = \frac{\rho_0 \alpha g \Delta T_0 h^3}{\eta_0 \kappa}, \quad (2.4)$$

where ρ_0 is a reference density, α the thermal expansivity, g the acceleration due to gravity, ΔT_0 a reference temperature difference, h the depth of the layer, η_0 a reference viscosity and κ the thermal diffusivity. It is not the aim of this paper to investigate the Nusselt–Rayleigh-number relation in detail. This has been done extensively by Christensen (1984, 1985). Nataf & Richter (1982) defined an internal Rayleigh number

$$Ra_T = (\rho_0 \alpha g \Delta T_0 h^3) / [\kappa \eta \langle T \rangle]$$

for the Bénard case with temperature-dependent viscosity η , where $\langle T \rangle$ is the actual average temperature. In the model of this paper (called K 149) we suppose a mantle mainly heated from within with temperature-dependent viscosity. In our code we have the option of a small, prescribed heat flow q_{CMB} at the lower boundary. The evolution of the temperature should be free at this boundary because there is no acceptable mechanism to keep the core–mantle-boundary temperature constant, whereas a feedback mechanism keeps the temperature constant at the surface of the Earth in spite of the growing solar luminosity. In analogy to Nataf & Richter (1982) we could introduce a Rayleigh number

$$Ra_Q = \frac{\rho_0 \alpha g h^4 (\langle Q \rangle h + q_{CMB})}{\kappa k \eta \langle T \rangle},$$

where k is the thermal conductivity and $\langle Q \rangle$ denotes the actual average heat-production density. Similar expressions have been discussed by Quarení & Yuen (1988) and Jarvis & Peltier (1989). We could of course use Ra_Q at a fixed time for scaling, but for numerical simplicity we used Ra . In this paper we assume a shear viscosity η dependent on the temperature T and the melting temperature T_m , where

$$\eta = k_1 \exp(k_2 T_m / T). \quad (2.5)$$

In other models, however, we suppose

$$\eta = A^{1/m} \hat{\epsilon}_{II}^{(1/m)-1} \exp(k_2 T_m / T) \quad (2.6)$$

or

$$\eta = A^{1/m} \hat{\epsilon}_{II}^{(1/m)-1} \exp\left(\frac{E_0 + PV_0}{nRT}\right), \quad (2.7)$$

where $R = 8.31441 \text{ J mol}^{-1} \text{ K}^{-1}$, $E_0 = 5.25 \times 10^5 \text{ J mol}^{-1}$, $V_0 = 6 \times 10^{-6} \text{ m}^3 \text{ mol}^{-1}$ and $n = 3$ (Kohlstedt & Goetze 1974). k_1 , k_2 , A are additional constants and P is the pressure, although we believe that the mantle is chemically inhomogeneous. The invariant $\hat{\epsilon}_{II}^*$ is defined by

$$\hat{\epsilon}_{II}^* = \left(\frac{1}{2} \hat{\epsilon}_{ik} \hat{\epsilon}_{ik}\right)^{1/2}. \quad (2.8)$$

In eqs (2.5) and (2.6), we always use $k_2 = 29$ and a melting-temperature curve obtained from Fig. 1 by joining the curves KJ, HJ and IT. In this way, we assume a melting temperature dependent only on the depth. The discretization of eqs (2.1) and (2.3) is performed by means of a finite-difference technique. Eq. (2.1), together with eqs (2.2), (2.3) and (2.5) have thus been used in this paper in order to compute the temperature T , the stream function ψ and the viscosity η as functions of x, z and time t . An additional redistribution mechanism for the $a_{\nu i}$ will be introduced in order to define the redistribution of the heat-producing isotopes caused by chemical segregation.

In this paper, we use a grid with 81×81 nodes and 161×161 tracers, which are regularly distributed in the initial state, as well as a box with an aspect ratio $a = 3$. For all numerical experiments reported in this paper, we chose stress-free boundaries. The surface is isothermal, the other boundaries have zero heat flux:

$$\begin{aligned} z = 1; & \quad 0 < x < a; \quad \psi = 0; \quad \nabla^2 \psi = 0; \quad T = T_c, \\ z = 0; & \quad 0 < x < a; \quad \psi = 0; \quad \nabla^2 \psi = 0; \quad \frac{\partial T}{\partial z} = 0, \\ 0 < z < 1; & \quad x = 0; \quad \psi = 0; \quad \nabla^2 \psi = 0; \quad \frac{\partial T}{\partial x} = 0, \\ 0 < z < 1; & \quad x = a; \quad \psi = 0; \quad \nabla^2 \psi = 0; \quad \frac{\partial T}{\partial x} = 0. \end{aligned} \quad (2.9)$$

T_c , converted into the dimensional variable, is 300 K. At a depth of 670 km, we fix the vertical velocity w as zero. The geophysical justification for this assumption will be given below.

As is common practice in numerical mantle-convection calculations, a small disturbance $T_s(x, z)$ is superimposed on the initial temperature $T_0(x, z)$ to set the flow in motion:

$$T_s(x, z) = A_s \sin\left(\frac{\pi x}{x_{\max}}\right) \cos\left(\frac{\pi z}{2z_{\max}}\right) T_m(z), \quad (2.10)$$

where $A_s = 0.01$ is used.

2.2 Internal heating and chemical segregation

Table 1 gives some material constants of the four major heat-producing radionuclides, calculated from the values of Van Schmus (1989). The abundances of the elements $a_{\nu i}$ (see Table 2) can now be introduced according to geochemical models. It should be noted that the present observed distribution of the radionuclides must be obtained only after the 4550 Ma of chemical and thermal evolution of the model Earth.

The trends of normalized concentrations of highly incompatible elements (Rb, U, Th, Ba, Cs, ...) and moderately incompatible elements up to the rare-earth elements within the

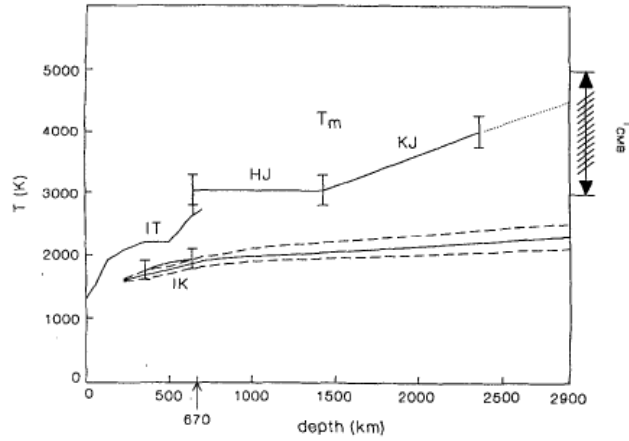


Figure 1. Melting temperature T_m in the mantle, compiled by Ranalli (1991). KJ, HJ: melting curve of perovskite (Knittle & Jeanloz 1989; Heinz & Jeanloz 1987); IT: dry solidus of peridotite (Ito & Takahashi 1987); T_{CMB} : the temperature at the core-mantle boundary (Leitch & Yuen 1989); IK: the lower-mantle adiabat and uncertainty (dashed lines) (Quareni & Mulargia 1989).

Table 2. The abundances a_{ij} of the major heat-producing elements according to Hofmann (1988).

Marker index	(1)	(2)	(3)	(4)	(5)
Reservoir	Primitive mantle (ppm)	Oceanic crust (ppm)	Continental crust (ppm)	Res 1 (ppm)	Res 2 (ppm)
K	258.2	883.7	9100	201.48	161.98
Th	0.0813	0.1871	3.5	0.0594	0.0529
U	0.0203	0.0711	0.91	0.0146	0.0112

continental crust show a clear negative correlation with the trends derived from MORBs. This indicates that the chemistry of MORB is related to the chemistry of the continental crust in a simple way. Various geochemical evolution models take this fact into account. We base our considerations on a modified *two-stage model* of Hofmann (1988). According to Hofmann, the primordial primitive mantle first differentiates into a continental crust and a first residue (res 1). Below, remnants of the primordial mantle are left. Then, from the first residue, the oceanic crust and a second residue are formed, and some remnants of the first residue are left over. In our fluid-mechanical model, we mark the geochemical contents of the different reservoirs by tracers.

Fig. 2 gives a diagrammatic view of the evolution scheme and the calculated volumes. The fully framed reservoirs would still be present today. The aim now is to introduce the first stage of chemical differentiation in a simple way into the differential equations for convection. One would actually have to introduce the degree of melting f and develop a two-phase convection theory, where

$$f \sim \frac{T - T_s}{T_l - T_s};$$

the subscripts 's' and 'l' stand for solidus and liquidus, respectively. We have, in fact, developed such a theory; however, in view of the computer capacity available, the numeric execution

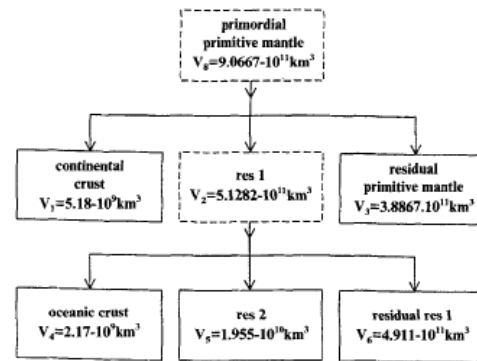


Figure 2. Two-stage evolution of the Earth. The reservoirs still existing today are shown with solid boxes; those no longer in existence, with dashed boxes.

will still take some time. In this paper, a simplified method is used. Markers (e.g. 161×161 markers for one run) are used to carry the information about the radioactive elements. Five types of markers are used, each type representing one reservoir (see Table 2). At first, the entire box with aspect ratio 3 is filled with type 1 markers (see Table 2). The box represents the homogeneous primordial mantle from which the continents, represented by type 3 markers, are to be formed. In a number of runs, we assume that, at the beginning of the evolution, the radioactive abundances of type 1 tracers for depths less than 670 km are increased by a factor k_8 (≥ 1) for all four nuclides. The choice of the factor k_8 is a geochemical starting assumption in order to arrive at the observed present average heat flow on the Earth's surface. The factor k_8 is defined in this way. Although $k_8 > 1$, for the present time of the Earth's evolution, this may nevertheless lead to a depleted upper mantle. If k_8

were 1 then it would be assumed that the whole mantle was originally homogeneous. In this paper, however, we use $k_8 = 5.512$, except in Fig. 8. The error bar of the present average heat flow allows a slight variation of the parameter k_8 . We examine the influence of a variation of this parameter on the evolution of the kinetic energy E_{kin} of the mantle convection. E_{kin} is a measure of the convective vigour. Although E_{kin} is the function most sensitive to the alteration of parameters, the curves of Fig. 8 are relatively stable. In an extended theory, it is necessary to introduce two velocity fields, one for the melt and one for the matrix. Areas with partial melting appear in places where the actual temperature surpasses the melting temperature of some minerals at the corresponding hydrostatic pressure. Using eq. (2.5) we can reformulate: areas of partial melt appear where the viscosity of the matrix drops below a certain critical value. Incompatible elements will be enriched in the melt according to the relevant partition coefficients, which are heavily dependent on the SiO_2 content.

To avoid the difficulties alluded to above, we suppose that the melt rises instantaneously and that the heat-producing incompatible elements are distributed in the geochemically observed ratios (see Table 2). Indeed, the rising velocities of magmas are orders of magnitude higher than the lithospheric-plate or solid-state convection velocities. The magma rises to the surface or to magma chambers near the surface that are situated in a plate of thickness D_c where, say, $D_c = 100$ km. In this way, a preliminary crust has been created. To avoid the additional magma hydrodynamics, we introduce an artificial tracer transformation that alters the density of the heat-producing elements in a similar manner. The movement of the matrix has been computed by the usual hydrodynamics, avoiding parametrized models, which have frequently been used in order to model the thermal evolution of the Earth (Schubert 1979; Christensen 1985; and many others).

We will now describe the algorithm of the simplified chemical fractionation. When the viscosity drops below a critical value η_{crit} in a sufficiently large area, we assume that the magma, enriched in heat-producing elements due to chemical differentiation, represented by marker transformation, is carried to the surface through volcanism. There, a number of type 1 markers are transformed into type 3 markers in a D_c -wide strip. The type 3 markers represent areas enriched in heat-producing radionuclides. The D_c strip is the future lithosphere. The type 3 marker piles on the surface represent the continents. The source region, on the other hand, is left depleted. Therefore, the type 1 markers in this region will be replaced by type 4 markers (see Table 2). A transformed marker near the surface represented originally an abundance $k_8 a_{\mu\nu}^{(1)}$; after the transformation it has a higher abundance, $a_{\mu\nu}^{(3)}$. The difference $a_{\mu\nu}^{(3)} - k_8 a_{\mu\nu}^{(1)}$ must be compensated by the transformation of $z_{\mu\nu}^*$ type 1 markers in the deeper segregation area. There, one of the original markers represented $k_8 a_{\mu\nu}^{(1)}$; it has been transformed into a marker with a lower abundance, $a_{\mu\nu}^{(4)}$. Therefore, the number of type 1 markers, $z_{\mu\nu}^*$, that is necessary to produce one continental marker (type 3) is defined by

$$k_8 a_{\mu\nu}^{(1)} + z_{\mu\nu}^* (k_8 a_{\mu\nu}^{(1)} - a_{\mu\nu}^{(4)}) = a_{\mu\nu}^{(3)} \quad (2.11)$$

and

$$z_{\mu\nu} = \text{round}(z_{\mu\nu}^*). \quad (2.12)$$

Eq. (2.11) serves as a description of the conservation of the numbers of parent and daughter nuclei during the chemical

segregation. Eq. (2.12) is necessary because the markers are indivisible. The numbers $a_{\mu\nu}^{(1)}$, $a_{\mu\nu}^{(3)}$ and $a_{\mu\nu}^{(4)}$ are the abundances given in Table 2 of the primordial mantle, continental crust, and first residuum, respectively. The first residuum is a part of the depleted mantle.

For readers wishing to use the idea of simplified segregation, some details of the code are described. If at the associated mesh point of a type 1 marker $\eta(T) < \eta_{crit}$ applies, then this marker is designated as a *type 1 marker with $\eta < \eta_{crit}$* . For each time increment, a rectangle of *minimum* height h_t is formed around each type 1 marker with $\eta < \eta_{crit}$. For η_{crit} we have always used 2.4×10^{20} Pa s. The ratio a_r of width to height, h_r , of the rectangle is fixed, e.g. $a_r = 2$. The reference marker is located in the centre. The following applies in the rectangle (including the boundary): {it contains exactly $z_{\mu\nu}$ type 1 markers with $\eta < \eta_{crit}$ [for $k_8 = 1$ in formula (2.11)] and these type 1 markers represent more than 50 per cent of the markers in the rectangle.} If no h_t can be found, one has to set $h_t = 10^{40}$ for a technical reason. For each individual time increment, the following will now be performed: for all h_t satisfying $h_t < 10^{40}$, the lowermost value is selected. Let this be $h_{t,min}$. If there is no $h_{t,min}$, we proceed to the next time increment. Otherwise: {all type 1 markers with $\eta < \eta_{crit}$ lying in and on the rectangle with $h_{t,min}$ are suddenly transformed into type 4 markers. The centre of gravity of the markers to be transformed is projected perpendicularly onto the surface. Let this point be designated as P' . The $rz_{\mu\nu}$ type 1 markers in the D_c layer ($D_c = 100$ km) situated next to P' are transformed into type 3 markers.}

The following also applies:

$$rz_{\mu\nu}^* = \frac{1}{6} \frac{z_{\mu\nu}^* [\text{for } k_8 = 1 \text{ from formula (2.11)}]}{z_{\mu\nu}^* [\text{for the given } k_8 \text{ from formula (2.11)}]},$$

or equivalently:

$$rz_{\mu\nu}^* = \frac{1(a_{\mu\nu}^{(3)} - a_{\mu\nu}^{(1)})(k_8 a_{\mu\nu}^{(1)} - a_{\mu\nu}^{(4)})}{6(a_{\mu\nu}^{(1)} - a_{\mu\nu}^{(4)})(a_{\mu\nu}^{(3)} - k_8 a_{\mu\nu}^{(1)})} \quad (2.13)$$

The number of the new type 3 markers is

$$rz_{\mu\nu} = \text{round}(rz_{\mu\nu}^*). \quad (2.14)$$

Apart from the rounding errors, this rule ensures the maintenance of the number of radioactive parent atoms and radiogenic daughter atoms.

A low and realistic thermal diffusivity κ_c ($\kappa_c = 0.6 \times 10^{-6} \text{ m}^2 \text{ s}^{-1}$) is assigned to the type 3 markers for the purpose of modelling the thermal blanketing effect of the continents. In addition to the constants mentioned above, the constants that were used in all the models have been summarized in Table 3.

The remaining parameters differ from model to model or from run to run and will be mentioned in the following. The non-dimensional stream function ψ is confined to values between 0 and 10^6 , and the temperature lies between 0 and 8000 K. The viscosity lies between 10^{17} and 10^{25} Pa s. This does not mean that these values are obtained in the model, but they are the cutting values in the code.

2.3 The 670 km discontinuity

Why do we assume that $w=0$ at a depth of 670 km? As is well-known, this depth is characterized by a discontinuity of the seismic velocities and by a sharp cutoff of seismicity

Table 3. Further model parameters

Parameter	Description	Value
h	Depth of the convecting layer	2.891×10^6 m
κ	Thermal diffusivity of the mantle	2.5×10^{-6} m ² s ⁻¹
κ_c	Thermal diffusivity of the continental crust	0.6×10^{-6} m ² s ⁻¹
α	Coefficient of thermal expansion	1.4×10^{-5} K ⁻¹
g	Gravitational acceleration	9.81 m s ⁻²
ρ_0	Density of the primordial mantle (type-1 markers)	3.984×10^3 kg m ⁻³
ρ_0	Density of the continental crust (type-3 markers)	2.900×10^3 kg m ⁻³
ρ_0	Density of res 1 (type-4 markers)	4.003×10^3 kg m ⁻³
c_p	Specific heat at constant pressure	1.26×10^3 JK ⁻¹ kg ⁻¹
ΔT_0	Scaling temperature contrast	3000 K

(Billington 1978). There are three possible reasons why we find a barrier to slab or/and plume penetration there: (1) phase transitions; (2) a viscosity jump; or (3) a compositional jump.

(1) An endothermic phase transition greatly diminishes the flow through the 670 km discontinuity. There, the seismic velocities increase by about 6 per cent. Zhao, Yuen & Honda (1992) realistically assumed that the 670 km discontinuity has to do with the location of the triple-point of the spinel to perovskite + magnesiowüstite phase transition. Plumes with temperatures lower than the triple point temperature cannot pass through this barrier because they are blocked by the multiple phase transition. They assumed that there is a negative Clapeyron slope at a depth of 670 km, e.g. -3.6 MPa K⁻¹. According to Akaogi & Ito (1993), the experimentally determined Clapeyron slope is (-3.0 ± 1.0) MPa K⁻¹. As a result, much heat is trapped in the lower mantle. The exact position of the triple point strongly depends on the exact iron content, which is not well known. Similar considerations can be found in Peltier & Solheim (1992). In a Cartesian model (Honda *et al.* 1993) and a spherical model (Tackley *et al.* 1993), the downgoing slabs are stopped above the 670 km discontinuity. The material forms huge piles, which penetrate into the lower mantle only after a long time. Unrealistically, younger models of convective avalanches in the whole mantle with shorter overturn periods presuppose constant viscosity. Ita & King (1994) have shown that a dynamic layering phenomenon is caused by the 670 km phase change.

(2) Other models contain a marked jump to a higher viscosity at this boundary (McKenzie & Weiss 1975). This is true also of the viscosity model TBL 1 discussed by Ranalli (1991, p.372). Our calculation results given below, however, show a very high viscosity only in the lower parts of the lower mantle. In the upper parts of the lower mantle, the viscosity decreases considerably on account of the heat accumulation at the 670 km discontinuity. If this boundary presents a barrier to slab penetration, then this is certainly not due to an *upward* viscosity jump. If there exists any viscosity jump in the geological present, then it is certainly directed downwards. Spada, Sabadini & Yuen (1991) have considered such a downward jump in the viscosity at $h=670$ km, albeit due to supposed chemical differences.

(3) A third possibility would be that of a sharp transition to a compositionally denser lower mantle. In earlier studies (e.g. Dickinson & Luth 1971; Ringwood 1975), the view was held that the lower mantle is the heavier residue of the chemical

differentiation, which leads to the formation of the continental material. Since the studies of O'Nions, Evensen & Hamilton (1979), Jacobsen & Wasserburg (1979), Jacobsen (1988), Allégre & Lewin (1989), Galer, Goldstein & O'Nions (1989), Hart & Zindler (1989) and other authors, the prevailing view is that the upper mantle is depleted, and largely transferred the aforementioned heat-producing elements to the continental crust through the formation of the oceanic crust at the mid-oceanic rifts during the first stage, and through the andesitic volcanism and plutonism at the subduction zones during the second stage. DePaolo (1988) has written an excellent textbook about these geochemical findings. With respect to the numerical values, our study is based on the two-stage hypothesis of Hofmann (1988). As a result of our computations we obtain for the present time a depleted upper mantle. But it is now evident that mantle convection is primarily driven by the heat sources and not by the small Rayleigh-Taylor instability.

In our models, we often obtain a step-wise increase in the viscosity in the transition zone. Thus, even if it is not assumed that there is an increased zero-temperature density or an increased viscosity below the 670 km discontinuity, the following can be stated: within the deep-focus zone, downgoing slabs are in a state of down-dip compression (Isacks & Molnar 1969), and the moment-tensor solutions and the seismicity distribution as a function of depth show thickening and bottoming out of the descending slab (Giardini & Woodhouse 1984). According to Ringwood's (1982) megalith hypothesis, the subducting slab buckles to form a mixture at the 670 km discontinuity so that in most cases there are no seismic extensions of the slabs.

2.4 Initial conditions

We assume that the starting temperature $T_0(x, z)$ of the Earth's mantle amounted to 70 per cent of the melting temperature $T_m(z)$, such that there was a lukewarm start. The reason for choosing such a temperature profile was to start the calculation with a moderate constant viscosity throughout the model. Moreover, we assume that there was a primordial source distribution, in accord with Hofmann (1988). In some models, we multiplied the abundances a_n for the start in the upper mantle by the factor k_8 so that the geophysical results obtained for the present will match better with the observations, taking great care to ensure that the four total amounts of long-lived radioactive isotopes (⁴⁰K, ²³²Th, ²³⁵U, ²³⁸U) were in agreement with those of Hofmann. Nevertheless, a depleted upper mantle

is obtained for the present, because the excess material has accumulated in the continental crust. Apart from the factors discussed above, the following plausibility considerations on the accretion of the Earth will not be incorporated in the model, but do contribute to the understanding of our assumption made above.

To come straight to the point: we believe that many essential questions of the formation of the Earth, including the question of a hot or cold formation, have not yet been sufficiently solved at the present time. Wetherill (1990) made a similar comment, pointing out that 'our understanding of all these events is, at best, rudimentary'.

Nowadays, the prevailing hypothesis is that the planets formed in several stages via planetesimals from the dust of the protosolar cloud (Schmidt 1957; Safronov 1969), as follows.

(1) First stage: presolar dust particles condensed from a molecular cloud.

(2) Second stage: larger clumps were formed from these dust particles through coagulation as a result of collisions at low relative velocities. These clumps were at first carried along by the rotating gas through viscous friction forces.

(3) Third stage: bodies measuring 1 to 10 km in diameter, the so-called planetesimals, were formed from these clumps. Their movement became disconnected from that of the gas, and they started to describe Keplerian orbits. (It was originally thought that the planetesimals were undifferentiated bodies of CI chondritic composition. Nowadays, there are good reasons to assume that the planetesimals were already differentiated bodies and that there were minor deviations from the CI chondritic composition.)

(4) Fourth stage: in zones with a high density of planetesimals, the disk became gravitationally unstable. Planet embryos grew.

(5) Fifth stage: in cases where the protoplanets (consisting of silicates, iron and sulphides) became significantly greater in mass than the Earth and sufficient quantities of hydrogen and helium or H₂O, NH₃, CH₄, CO and N₂ were present in their surroundings, giant gaseous planets or icy planets were formed. The latter mechanism is controversial. While Mizuno (1980) assumed that, after a so-called critical mass was reached, a sudden collapse took place due to gravitational instability and that the surrounding gas masses accreted relatively quickly to the nucleus resembling a terrestrial planet, Wuchterl (1989) calculated that the suggested κ -mechanism eventually leads to an explosion of the object.

The Earth has not gone through this fifth stage. We have mentioned it here in order to emphasize that the speed of the fourth stage does not have to be so high that thereby the accretion of Jupiter, Saturn, Uranus and Neptune could have taken place in a sufficiently short time.

The hypothesis that the planets have formed rapidly and, so to speak, without going through different stages, through giant gaseous protoplanet instability, and that the solar wind of the T-Tauri phase has robbed the terrestrial planets of its atmosphere (Cameron 1978), a formerly widespread hypothesis, is nowadays rightly dismissed (Cameron 1988; Wetherill 1990; Boss 1990).

Let us now discuss the fourth stage of the standard evolution model mentioned above. According to Safronov (1962, 1969), the relative velocities of the planetesimals must not be treated

as free parameters. The velocity distribution is determined by the mutually perturbing planetesimals. If a protoplanet grows through collisions with comparably sized other planetesimals, it will grow relatively slowly through orderly growth (Safronov 1991). As the protoplanet to planetesimal mass ratio increases, runaway growth occurs (Wetherill & Stewart 1993; Ida & Makino 1993). Whether the Earth has developed slowly, not just in the beginning but generally, and whether runaway growth has or has not only occurred in the giant planets depends on the size of the available building blocks and on the path parameters (eccentricity, inclination, etc). In the case of slow growth, the Earth may have formed at relatively cool temperatures, while this is not so in the runaway case. Also, with heterogeneous accretion a combination is conceivable whereby the inner core slowly formed first, whereupon, accompanied by strong heat storage, the outer core formed through runaway growth. The silicate mantle could then have formed without any significant melting by a slowing down of runaway growth (Ida & Makino 1993). In this case, it has to be assumed, though, that a chemical differentiation took place in the protoplanetary cloud. At present, authors are somewhat more in favour of the hot formation of the Earth. Cameron & Ward (1976) suggested that the Moon has come into being as a result of a collision of the primordial Earth, which was differentiated into an iron core and a silicate mantle, with a body about the size of Mars. Newsom & Taylor (1989) concluded that the hypothesis is geochemically acceptable. It is quite obvious that the Mars-sized body would have vapourized part of the Earth and would have melted the rest of it (Melosh 1990; Benz & Cameron 1990). Another source for the assumption that the primordial Earth was hot are the attempts made to explain the formation of the iron core of the Earth from an originally homogeneous iron-silicate mixture in the case of homogeneous accretion. Arculus *et al.* (1990) underlined the fact that the separation of liquid iron from a solid silicate matrix is unlikely due to the high surface tension of the metal. For low pressures, as in the case of the Moon and the eucrite parent body, an extensively molten silicate magma ocean would be necessary for achieving the segregation. A segregation with a fixed matrix under a high pressure appears to be even more improbable. Stevenson (1990) developed a mixed model with an iron pond at the bottom of a magma ocean, *not* comprising the whole mantle, and leaky diapirs seeking their way through the partially solid deep mantle, on the one hand, and percolation of iron through the deep mantle, on the other hand. Lunar samples and meteorites show that the upper few hundred kilometres of all terrestrial planets were molten (Warren 1989). The Kyoto variant of the standard model of planetary accretion mostly leads to planets having a magma ocean in the beginning. Because of the blanketing effect, a primordial atmosphere rich in mass leads to a high temperature at the bottom of the atmosphere. When the planet has reached 0.3 Earth masses, the iron core is formed simultaneously with the accretion of the planet (Mizuno & Nakazawa 1988). In contrast to Warren (1989) and Mizuno & Nakazawa (1988), the proponents of the giant impact naturally have to proceed from the assumption of a total chemical stratification of the Earth's mantle. This is the case with Agee (1990), for example, whose mantle model, as seen from the bottom to the surface, is layered as follows. At the bottom of the lower mantle, there is magnesio-wüstite, a large portion of it also being dissolved in the outer core. Mg-perovskite is predominant in the main

part of the lower mantle. It is followed by a komatiite shell, topped by a peridotite shell. Agee holds the view that the composition of the layers may not be identical to that in the present Earth, and that everything may have become mixed through solid-state convection. Our convection calculations have shown that the ability of the convection flows to mix chemical reservoirs relatively quickly is overestimated.

According to Ringwood (1990), the chemical stratification of an initially molten mantle consists of MgSiO_3 perovskite and $(\text{Mg,Fe})\text{O}$ in the lower mantle, aluminium-rich garnet and γ , β $(\text{Mg,Fe})_2\text{SiO}_4$ in the transition layer, and olivine and omphacite in the upper mantle above a depth of 400 km. The buoyant primitive crust, according to him, is about 30 km thick and consists of alkali feldspar and nepheline as the major phases. The known continental crust, which has been in existence for 3.8 Ga, however, has a completely different composition. Ringwood finds it hard to understand why no remnants of the primitive crust should have survived. The high abundances in the upper mantle, confirmed by many investigators, of Ni, Co, Cu, Re, Au, Ru, Rh, Pd, Os, Ir and Pt, occurring in approximately primordial Cl proportions, also indicate that the upper mantle was never in thermodynamic equilibrium with the core. Cr, V and Mn are lithophiles at lower pressures in a Martian-sized planetesimal. At the higher pressures prevailing in the Earth, they would become siderophiles. Cr, V and Mn are depleted by factors of 0.6–0.2 in the Earth's mantle and the Moon, but undepleted in the Martian mantle and the eucrite parent body. Therefore, though it might be possible that the Moon originated from the Earth's mantle, there was no giant impact of a Martian-sized body. Extensive melting of the whole Earth is out of the question. Consequently, it would make sense to assume that the temperature at the start of the evolution of the Earth was somewhat lower than the melting temperature.

The question as to the chemical composition of the Earth has been solved much better than the question of the temperature prevailing at the beginning of the Earth's evolution. Since the abundances of Cl chondrites and of the solar photosphere show quite good agreement for the non-volatile elements, the majority of authors held the view that the Earth on average is of chondritic composition. This view needs to be modified, however. The deviations the Cl chondrite data show from those of the solar photosphere and corona amount to ± 5 –10 per cent. Yet, Anders & Grevesse (1989) found greater discrepancies for Fe, Mg, Ge, Pb and W. More recent investigations into the solar photospheric spectral data have again demonstrated the coincidence between Cl and solar photospheric iron values (Holweger, Heise & Kock 1990; Biémont *et al.* 1991). There must have been a certain chemical inhomogeneity in the solar nebula. Kerridge (1993) goes even further, emphasizing that the least-metamorphosed ordinary chondrites are petrologically at least as primitive as carbonaceous chondrites. In the asteroid belt, a rapid decrease in the degree of chemical differentiation of bodies with extensive melting and magmatic differentiation towards undifferentiated bodies further away from the sun is observed. At 2.0 AU, 100 per cent of the asteroids are igneous bodies; at 3.5 AU, however, 0 per cent are igneous bodies (Gaffey 1990). The conclusion that the Earth was formed from planetesimals with iron cores suggests itself. This metal-sulphide-silicate equilibrium was mainly established at low pressures and in low gravitational fields (Taylor 1992). The cause of the strongly decreasing tendency

to segregation in the outward direction (as seen from the sun) is not clear. Short-lived radioactive isotopes such as ^{26}Al should, after all, be more uniformly distributed. Therefore, it is electrical induction during the early T-Tauri and FU Orionis stages that comes into question, since this would provide an explanation for the decrease in the outward direction. Whereas Kargel & Lewis (1993) suggested a new best bulk silicate earth model and concluded that the bulk Earth's volatility trend closely resembles the average composition of H chondrites (H3–H6), Taylor (1992) holds the view that the well-known specific classes of meteorites do not include any suitable building blocks for the Earth. However, there can be no doubt that the inner planets have a general chondritic composition.

In order to have a specific model as a starting point for our calculations, we largely follow the Mainz group. Jagoutz *et al.* (1979) have determined the chemical abundances in the Earth's mantle from primitive ultramafic nodules. As we are mainly interested in the abundances of U, Th and K, the study of Jochum *et al.* (1988) is of particular interest. These data have also been used by Hofmann (1988).

The chemical differentiation model that we have translated into dynamics makes use of the abundances of the geochemical reservoirs of Hofmann (1988). The existence of geochemical reservoirs has been recently proven (Hart 1988). If the normalized concentration is plotted against the compatibility of the chemical elements, the continental crust and MORB show a complementary relationship for highly and moderately incompatible elements, while the concentration uniformly decreases for the only slightly incompatible elements. In this way, a maximum is created for MORB. This maximum lies at intermediate to heavy REE, Zr, Hf, Y, Ti and Na. Maximum abundances for Cs, Rb, Ba, U and Th are found in the continental crust. The latter are of particular interest to us in connection with the internal heating of the Earth. The distribution of the elements in the geochemical reservoirs can be explained by two stages. A partial melt was extracted from the mantle at an early stage. From this melt, the continental crust was formed. The effective aggregate melt fraction required for this purpose amounts to only about 1.5 per cent. The residual mantle (res1) is rehomogenized. Later, MORB was formed from res1. The concentration maximum of MORB may be explained best by a melt fraction of 0.045. The retention of Ca, Al and Sc in MORB is worth noting. Only aluminous clinopyroxene can retain these elements. Therefore, the degree of melting of MORB must be low in order to ensure that the clinopyroxene survives. Consequently, we will have only partial melting here and thus no complete melting. In his model, which does not involve any genuine dynamics in our sense, Hofmann uses the batch melting equations to construct the model. It is obvious that this does not provide a definition of the exact nature of the melting process. It does not become very clear whether the partial fusion comes closer to the model of batch-melting or to the model of fractional (or Rayleigh) melting. It is evident, however, that partial melting is much more probable than total melting. This is in agreement with our assumption of an initial temperature in the Earth's evolution that is lower than the melting temperature, so that our dynamic model is compatible with Hofmann's geochemical conclusions.

Wänke, Dreibus & Jagoutz (1984) also pointed out that the existence of almost primitive mantle reservoirs, as evidenced by primitive xenoliths, means that the amount of melt was

small. Perhaps the melt was present in the form of a trapped liquid in the solid matrix. This is another indication that the initial temperature should be expected to be somewhat below the mean of the melting curves of the mantle minerals.

3 RESULTS

All results given below relate to the model K149 described above. Fig. 3 gives an overview of the temporal development of our mantle model since the accretion of the Earth. The present-day mean heat flow on the surface of the Earth is 101 mW m^{-2} for oceans and 65 mW m^{-2} for continents. The global mean of the present heat flow is 87 mW m^{-2} (Pollack, Hurter & Johnson 1993). This shows good agreement with the heat flow q_{ob} averaged over the model surface. The first panel of Fig. 3 furthermore shows that the global mean of the heat flux has been monotonously falling for 3900 Myr, while the mean temperature of the mantle has been approximately constant for 3000 Myr (see lower panel). As we have taken the initial temperature of the Earth to be lukewarm, an assumption substantiated in Section 2.4, we have a slight heating in the

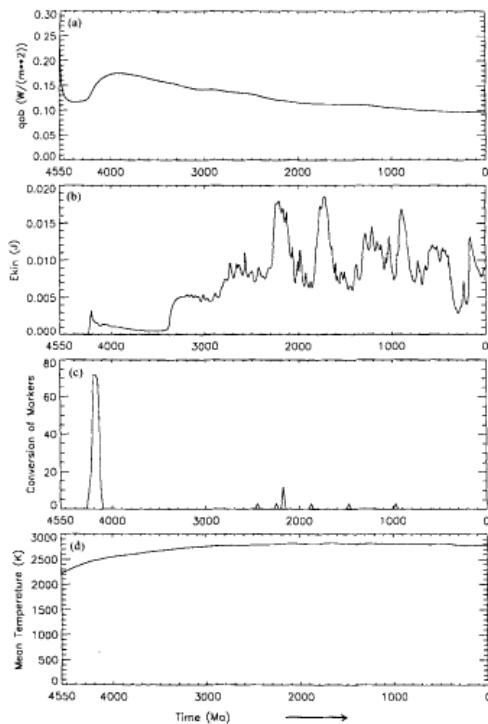


Figure 3. Time-series of the evolution model of thermal mantle convection with chemical segregation of the continental crust from the primordial mantle. (a) The heat flow q_{ob} averaged over the surface of the Earth; (b) the kinetic energy of convection averaged over the whole mantle; (c) conversion of markers of new formation of continental crust; (d) temperature averaged over the whole mantle.

beginning. Archaean komatiites have a high MgO percentage in comparison with Proterozoic picrites. On this basis it has often been concluded that the Archaean mantle was about 300 K hotter than at present. On the other hand, the Archaean geothermal gradients are recorded in widely distributed Archaean metamorphic rocks. They are equal to or only slightly higher than today (Wells 1976; Burke & Kidd 1978; Bickle 1978). Therefore, the mantle temperatures have been equal to or only slightly higher than today's if the surface temperature is considered to be constant. If the lateral upper-mantle temperature differences were greater than at present both observations could be explained.

The third panel of Fig. 3 shows that the chemical segregation of the continental material in the model essentially took place 4200 Myr ago. What this refers to is the net growth through time of the total continental crust, and it should not be mixed up with the growth of individual continents by accretion of island arcs and terranes, etc. This, as well as the regional metamorphism and anatexis (i.e. a kind of recycling), determines the mineral date abundances, which are quite irregularly distributed with various maxima and minima over the entire age of the Earth. In this way, a mean age of the rocks of the continental crust of approximately 2 Ga is obtained (Jacobsen & Wasserburg 1979; Hofmann 1988). We shall discuss these variations in the rejuvenation rate of the continental crust below in connection with Fig. 9. There exist quite different recycling mechanisms (Armstrong 1981; Meissner 1986), which lead to the transformation of the continental crust. On the ordinate of panel 3 the conversion of type 1 markers (in number of markers per 25 Myr) is shown. There is a linear relationship between this number and the newly depleted mantle volume. The whole primordial mantle volume is represented by 161×161 markers.

The vast bulk of the continental material must have already been created during the earliest Archaean (Warren 1989). At the time of the filling of the lunar mare, i.e. 3700 Myr ago, a 50 to 75 km thick lithosphere must already have existed on the Moon. Dasch, Ryder & Nyquist (1988) have come to the conclusion that the main era of lunar crustal genesis was 4500–4200 Myr ago. According to Warren (1989), such a mechanism was effective on the Earth at the same time. Kröner (1985) concluded that the growth of the continental crust took place at a much higher speed in the Archaean than later on and that up to an age of 2500 Ma more than 70 per cent of the continental crust had formed, a conclusion that does not contradict the preceding considerations. Hofmann (1988) does not define any fixed point of time, but opts for a two-stage model, in which the continental material is extracted first, while the process of the formation of the oceanic crust sets in only at a later date. According to our model, the main period of the formation of the continental crustal material was 4300–4100 Ma.

The second panel of Fig. 3 shows the evolution of the kinetic energy of the convective flows of the whole mantle in our model. It is reckoned per unit length in the y -direction. Although the kinetic energy is negligible in mantle convection, its variation with time may serve as a measure of convective vigour. Even if the input parameters are varied slightly, the general nature of the E_{kin} curve behaviour is quite stable (see Fig. 8). The early Archaean, more than 3400 Myr ago, was characterized by upper-mantle convection. The lower mantle was only gradually heated at this time until the critical Rayleigh

number was reached. The Proterozoic and Phanerozoic are characterized by considerable variations of the kinetic energy of the flow at a higher average of the energy level than during the Archaean. From an age of 3400 Ma onwards, there is thermal convection both in the upper and lower mantle, with the lower, deeper part of the lower mantle reacting only very sluggishly. The greater maxima in the E_{kin} curve are produced by vigorous movements in the upper half of the lower mantle and in the upper mantle.

The initial heating of the lower mantle also becomes evident in the temperature distributions shown in Fig. 4. While the upper mantle exhibits a multitude of convection cells, two cells have been developing in the lower mantle since an age of 3400 Ma, the downward stream being situated at the lateral edges. It is clear that these edges are an artificial feature of the model. The development of the streamfunction ψ in Fig. 6 underlines the foregoing considerations.

The shear viscosity in the model, being neither spatially nor

temporally constant, shows a dynamic development (see Fig. 5, left side). It has a strong influence on the velocity field. When averaging for a fixed depth over the whole mantle, we obtain the evolution of the viscosity–depth profile shown at the right side of Fig. 5. The 670 km discontinuity is present at all times as a barrier of increased viscosity between the upper mantle and the higher part of the lower mantle. Consequently, a subducting slab must experience a mechanical resistance there. Fig. 6 compares four snapshots of the streamlines of mantle convection.

Fig. 7 shows the change in the chemical composition of the mantle. For reasons of space we have confined ourselves to three snapshots, including the ages 3719.9 Ma, 1606.3 Ma and -0.1 Ma (i.e. practically the geological present). The first panel shows a lithosphere with superimposed continental crust. A depleted upper mantle has already developed below the lithosphere. Due to convection, the distribution of the radioactive sources has a tendency towards irregular schlieren forma-

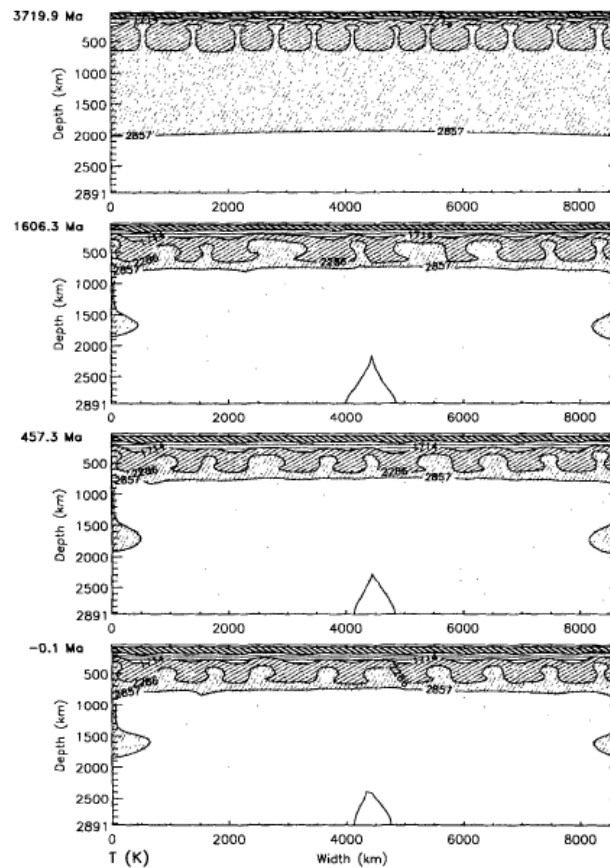


Figure 4. Evolution of the temperature field. Time advances downwards. The age of the snapshots is given on the left-hand side of each panel. The numbers on the isolines designate the temperature in K.

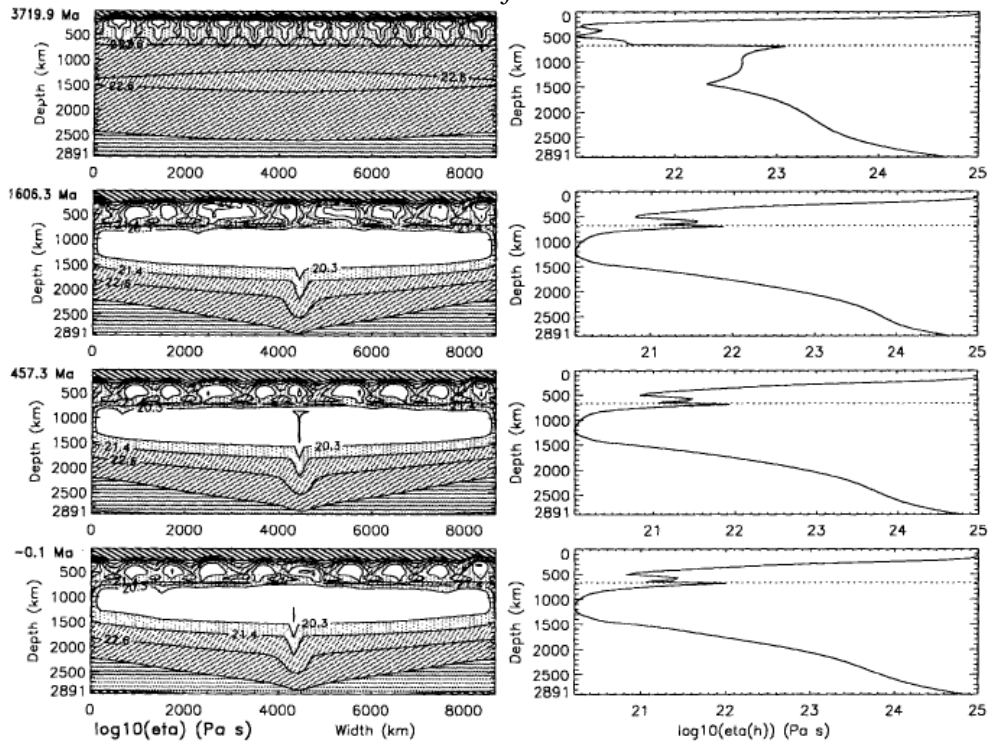


Figure 5. The left side shows a series of snapshots of the shear viscosity calculated in Pa s of the model mantle; the right side shows the viscosity, averaged over the entire width, as a function of the depth.

tion. The lower mantle does not show any convection in the first panel, representing a date in the Archaean. Therefore, the tracers are still in the initial position. On the other two panels of Fig. 7, the lithosphere has developed distinct undulations at its lower face. The depleted upper mantle has been preserved. The convection in the upper and middle parts of the lower mantle causes small-scale irregular scattering of the tracers. Remnants of the regular initial distribution of the markers in the lowermost part of the lower mantle indicate the presence of insignificant flows due to a very high viscosity. If, in addition, there are such plumes (not incorporated here in the model) ascending in ~ 100 km diameter tubes from the D'' layer through the lower mantle and causing hot spots in the lithosphere, a frame would be provided through the highly viscous lowermost part of the lower mantle, which would explain the immobility of the hot spots.

For the Archaean, our model (see Fig. 5) has relatively high viscosity values in the lower mantle. For the present, the same applies only for the lowermost part of the lower mantle. This is in contradiction to the value of 30×10^{21} Pa s that has recently been proposed for the present lower mantle. Schubert (1979) has emphasized that lower-mantle viscosity values of about 10^{21} Pa s would cause such efficient mantle convection that it would lead to core freezing. Schubert & Young (1976)

found that the lower-mantle viscosity must be in part greater than 10^{23} Pa s in order to prevent the core-mantle-boundary temperature dropping significantly below the iron melting temperature. Schubert (1979) stressed that there are several ways to prevent core solidification. One way would be a significant radioactive core heating, but this has only a low probability for geochemical reasons. Schubert (1979) also wrote: 'another way is to prevent convection from reaching the lower mantle for a portion of the Earth's history, particularly during the initial period of cooling after core formation when convection should be especially vigorous.' In our model, only the upper mantle convects during the early Archaean more than 3400 Myr ago, whereas later on, the material flows in the upper *and* the lower mantle.

In his excellent paper, Schubert (1979) started with a hot Earth at the beginning of the evolution because he supposed that the gravitational potential energy made available during accretion and core formation is the most important energy source for the Earth. Therefore, Schubert, Cassen & Young (1979) modelled the thermal history of the terrestrial planets by a parametrized calculation without any energy sources other than an initial thermal energy resulting from accretion and core formation. The thermal history was thought to be only a monotonous cooling. Schubert was convinced that, also

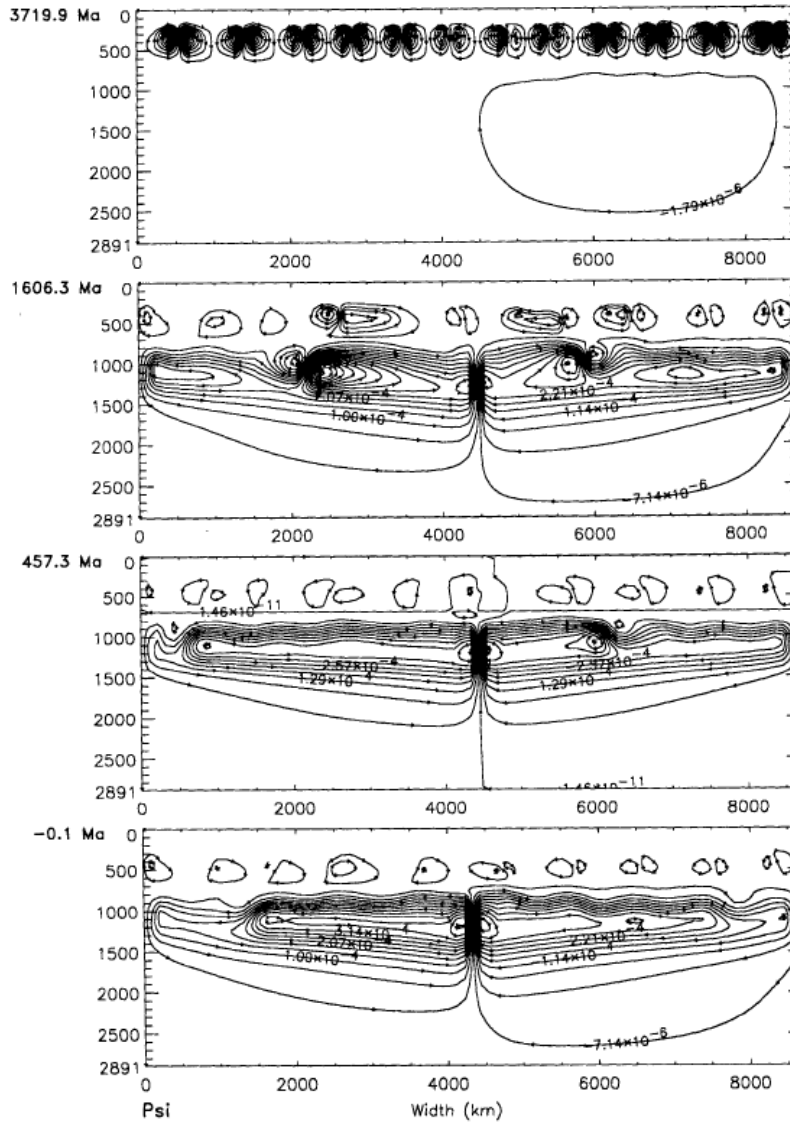


Figure 6. A series of snapshots for the streamlines. The direction of the flow around streamlines with negative psi values is clockwise, that around streamlines with positive values is counterclockwise. The units are given in $\text{m}^2 \text{s}^{-1}$.

taking into account the radiogenic heat sources, the thermal history of the Earth is only a history of cooling. It is very probable that the precursor objects of the Earth were planetesimals. These objects were melted before the accretion of the Earth and therefore already had metallic cores and silicate mantles (Taylor 1992). In scenarios of the Earth's accretion

from smaller bodies, the heat from impact is re-radiated to space. If one layer or other part of the primordial Earth is made up of large planetesimals or of one large object, the layer or part will be molten at the beginning. The high abundances in the present upper mantle of Ni, Co, Cu, Re, Au, Ru, Rh, Pd, Os, Ir and Pt show that the upper mantle did not achieve

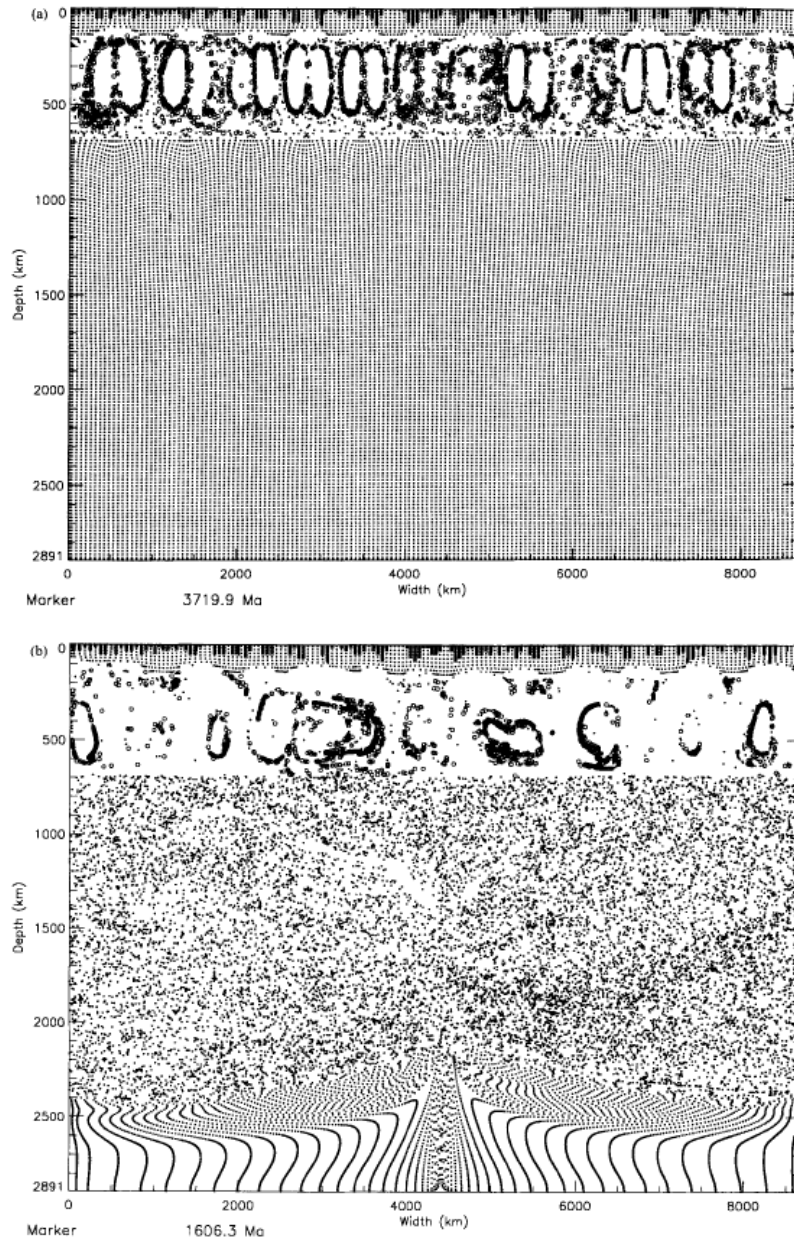


Figure 7. The development of the chemical composition of the mantle. Simple dots represent the primitive mantle, asterisks are for the continental crust and small circles for the depleted mantle (res 1). Refer to Table 2.

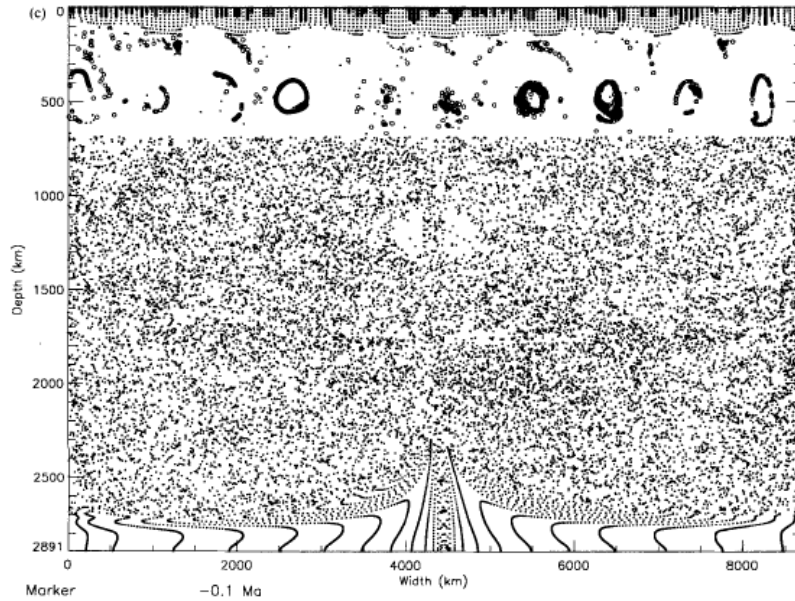


Figure 7. (Continued)

equilibrium with the core. Therefore, the late accretion of CI planetesimals is the usual explanation for the high abundances of the aforementioned elements. Taylor & Norman (1990) used a graphic comparison: 'the late infall of planetesimals to planets, which are essentially complete, is like adding icing to a cake; the decoration may give little insight about the composition of the interior.' Therefore, and for other reasons summarized in Section 2.4, we introduce a mantle convection model with two layers and a lukewarm thermal starting condition. In contrast to Schubert, we do not use a parametrized convection model but a genuine dynamical approach. Further, we introduce geochemical segregation dynamics based on modern numerical values for the abundances of the heat-producing radionuclides. The new model has some features in common with the Schubert model, while other features deviate. It is evident that our 2-D model may be unstable to perturbations in the third dimension. In common with Schubert, we hope that average values of the model, for example the mean surface heat flux q_{ob} or the mean temperature, give results similar to the 3-D problem.

In both models, the mean surface heat flow q_{ob} falls slowly and monotonously from 4000 Ma and arrives at the observed present value (see Fig 3, first panel). In our model we have a relatively short increase of q_{ob} before 4000 Ma, whereas Schubert's model has a strong decrease of q_{ob} at that time. In both models, there is almost no alteration of the average mantle temperature during the last 2000 Myr, in our model even during the last 3000 Myr. Before that time, the average temperature increases slightly in our model and it decreases strongly in Schubert's parametrized model.

Archaean komatiites have an MgO content between 18 and

28 per cent. The maximum value corresponds to a liquidus of 1576 °C, whereas Phanerozoic komatiites, which we know only from one locality, have 18 to 19 per cent MgO with a liquidus of 1417 °C (Abbott & Mooney 1995). This fact has often been explained by higher temperatures of the entire Archaean upper mantle and is thought to be the only direct proof of a hot accretion of the Earth. We believe, however, that the Archaean upper mantle had laterally very different temperatures because of the very different size of the planetesimals: small ones brought almost no accretion heat; where large objects fell a large amount of accretion heat was stored. Furthermore, we believe that the Archaean komatiites are biased samples. Komatiites appear to be hot-spot magmas. First, they must not be considered as representative samples for the bulk mantle. Second, the variation span of the MgO content of Archaean komatiites between 18 and 28 per cent corresponds to a lateral variation of the liquidus between ~1417 and ~1576 °C at that time. On the other hand, a fully non-layered convection model would result in an upper mantle that has been in equilibrium with the outer core. It would be unable to explain the high amount of platinum-group elements in the present upper mantle. Graham *et al.* (1996) came to the conclusion that there is only an insignificant mass transport (at certain places) from the lower mantle across the 660 km seismic discontinuity. This assumption is also necessary to explain the persistence of the commonly accepted high $^3\text{He}/^4\text{He}$ reservoir located in the lower mantle. In our model, different geochemical reservoirs have evolved that have the proper size and the observed amount of radiogenic heat sources. We want to emphasize that we do not use a uniform heat source distribution. In contrast to the most parametrized mantle

convection models, we obtain a non-monotonous kinetic energy versus time curve, so we are able to explain in principle the fluctuations of the global magmatism and the Wilson cycles. We agree with Bunge, Richards & Baumgardner (1996) that the influence of even the strongest phase change is minor in comparison with that of the viscosity.

The anonymous reviewer of this paper noted that Schubert (1979) has proved 'that a convecting mantle has no memory of its initial conditions, i.e. no matter if it started hot or cool, it would have arrived at the same state today.' We believe that this is not the whole truth. Because of the paramount importance of the temperature dependence of the viscosity, the mantle acts as a thermostat in the first approximation. It can be observed in Schubert's *and* in our model that the present mean temperature is rather insensitive to the initial temperature. On the other hand, we must not forget that Schubert, too, presented only a model (as did we) and that his conclusions depend on his model. We believe that the incorporation of more geochemical details will allow us to decide in the future whether the initial conditions of the Earth were hot or cold or lukewarm. We have carried out a first step in this direction. Schubert (1979) did not include any geochemical considerations. Nowadays we can possibly disentangle even the different fractionation processes of the Earth's evolution (gas-dust differentiation in the nebula, fractionation of planetesimals, Earth core formation, differentiation of the Earth's crust, etc.) by use of the radiogenic daughter isotopes of the extinct radionuclides ^{129}I , ^{244}Pu , ^{146}Sm , ^{182}Hf , etc. Using our geodynamical model, we arrived at a depleted upper mantle, acceptable values near to the observed heat flow, and acceptable distributions of temperature, viscosity and creep velocity in the mantle. The peaks and minima of the convective vigour curve of the model roughly resemble the supercontinental cycles, the worldwide distribution of mineral date abundances in time, the sea-level variations and the variations of a number of geochemical parameters, whereas most parametrized models, for example Schubert (1979), have no peaks and minima in their evolutionary curves. The E_{kin} curve depends on the initial temperature distribution but it has an island of stability against a variation of the starting distribution. Of course, the fact that the results of our model are similar to the observational results does not prove its validity, but this also applies to other geophysical models and their conclusions.

The influences of the variation of the parameters are noticeable in the main in the kinetic energy. Therefore, by way of example, we wish to show here the effect of the amplification factor k_B on the kinetic energy (see Section 2.2). Fig. 8 shows for a variation of k_B that the general appearance of the E_{kin} curve and also the approximate frequency content do not change so that the general statements given above in respect of this curve may also be transferred to other k_B in the vicinity.

Fig. 9 is a first attempt to venture a comparison of our model with significant geological observation data. Naturally, no exact agreement of the phases may be expected, since our model is strongly simplified in several respects. At the bottom of the figure, the worldwide distribution of the mineral date abundance is plotted against the age. It is assumed that while for a more modern compilation the relative height of some maxima would change, this would not be the case for the fundamental character of the distribution. It can easily be seen that the frequency content resembles that obtained when the

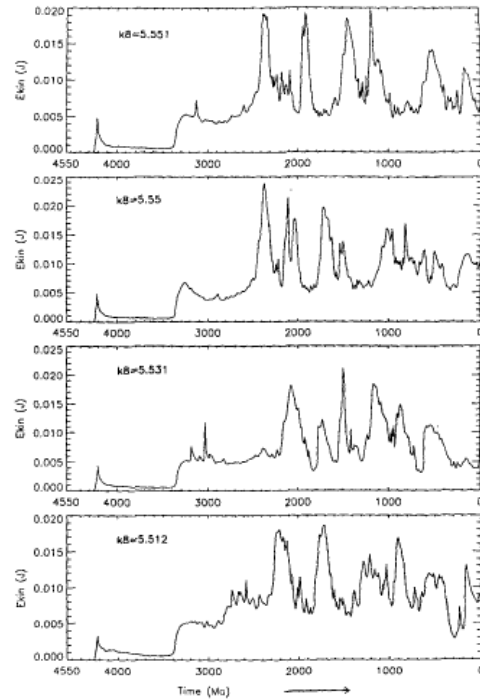


Figure 8. A variation of the amplification factor k_B has only a minor influence on other variables, the largest being on the dependence of the kinetic energy of the mantle convection on the time. The latter is shown for a number of k_B values.

kinetic energy of our mantle model is plotted as a function of time.

To avoid misunderstandings, it should be pointed out that our episodes with an increased kinetic energy of the mantle flow, which become apparent in the form of episodically (and, thus, not strictly periodically) distributed Wilson cycles and increased magmatic and orogenic activity in the continents, cover a considerable time span. They should by no means be mistaken for Stille's (1944) *short-time* rapid worldwide orogenic episodes. Whether these actually exist (Rampino & Caldeira 1993), or whether the individual orogeny is a continuous process, and angular discordances are only mistaken at certain locations for episodes of deformation (Şengör 1990), is of secondary importance and will not be discussed here.

Titley (1993) has shown that strata-bound Phanerozoic metal-sulphide ore deposits are closely linked with certain events of the Wilson cycle. He was able to demonstrate particularly well for volcanogenic massive sulphide (Cu, Pb, Zn) ores that their occurrence is tied to high sea levels in the Wilson cycle. He mentions an attempt to construct Proterozoic Wilson cycles on the basis of Windley's (1984) descriptions. In Fig. 10, this hypothetical sea-level curve (at the bottom) is compared with $E_{\text{kin}}(t)$ curves of our model (at the top). In the dotted rectangles underneath, the principal dyke swarms are

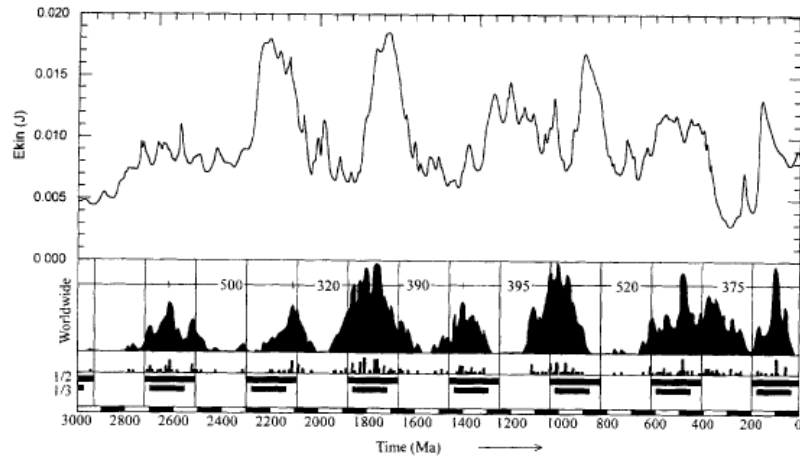


Figure 9. A comparison of the kinetic energy of the mantle convection (this work) with a plot of mineral date abundance against age according to Gastil (1960). This comparison is not intended as proof of the identity of the phases, but as an indication of the resemblance of the frequency content of both curves.

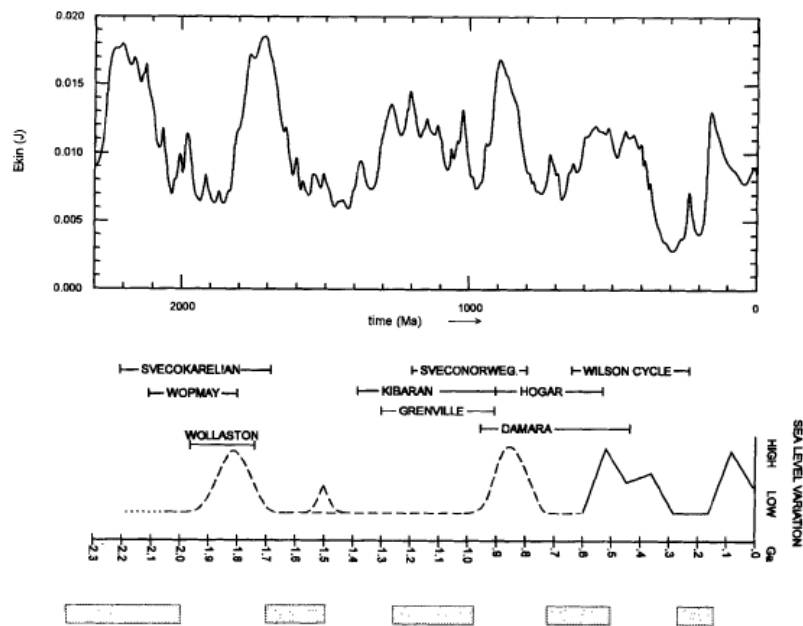


Figure 10. Comparison of the sea-level variation after Titley (1993) (shown in the bottom part of the diagram) with the variation of the kinetic energy of mantle convection (this work, upper part of the diagram).

shown for the purpose of comparison. It can clearly be seen that the behaviour of the curves shows some similarity.

Fig. 11 compares the time dependence of the kinetic energy of mantle convection from our model (at top) with the mag-

matic rocks of the highest MgO content from Campbell & Griffiths (1992). The maximum MgO content of magmatic rocks from Archaean greenstone belts lies at around 32 weight per cent. Between 2700 and 2000 Ma, an abrupt change to

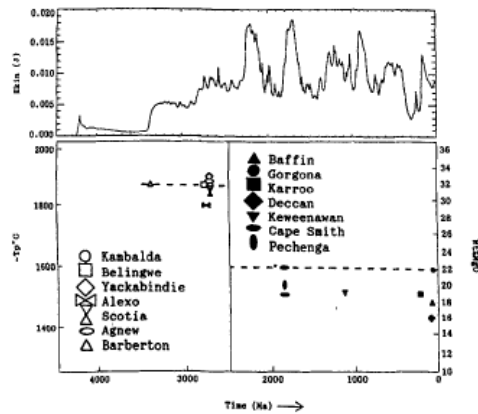


Figure 11. Comparison of the kinetic energy of mantle convection (top) (this work) with the variations in the maximum MgO content of komatiites and picrites after Campbell & Griffiths (1992).

values between 16 and 22 weight per cent MgO content of post-Archaean picrites takes place. We explain this change, which was also noticed by Campbell & Griffiths, in terms of the beginning of the large fluctuations in the E_{kin} curve. The latter, as can be seen from the tracer figures (Figs 7a to c), are due to the fact that the deeper parts of the mantle also start to convect.

The assumption that the primordial mantle was chemically completely homogeneous is probably a fictitious one, on which our model does not have to rely, since the chemical assumptions used in the calculations relate only to the radiogenic heat sources. It is our view, therefore, that the different depths of the lower mantle differed in the beginning in their MgO contents, and that material with a low MgO content was transported through convection from the deeper into the shallower parts of the lower mantle. The reinterpretation of the MgO contents in terms of potential temperatures T_p , which are shown on the left side of Fig. 11, and which have been calculated using the methodology of McKenzie & Bickle (1988), is not convincing. Although the komatiitic or picritic magma may have been transported upwards through plumes, the sources of the mantle plumes need not necessarily have been located in each case on the core-mantle boundary.

Fig. 12 shows for the Phanerozoic a comparison of our E_{kin} curve (top) with the stable isotope records of carbon (Veizer, Holser & Wilgus 1980) and sulphur (Claypool *et al.* 1980), the $^{87}\text{Sr}/^{86}\text{Sr}$ ratio (Burke *et al.* 1982; Veizer *et al.* 1983) and the schematically simplified record of freeboard after Worsley, Nance & Moody (1984), designated 'model' in the figure. Since the Wilson cycle influences the climate, in particular the degree of markedness of the climatic zones, evaporites occur more frequently during certain periods. Periods of extensive evaporite formation are characterized by a decrease in the total supply of isotopically heavy sulphur. Remains of living organisms contain higher amounts of isotopically light carbon. Since the amount of these remains also varies with climate, a correlation of the $\delta^{13}\text{C}$ curve with the E_{kin} curve makes sense. In addition, a direct connection with mantle convection may

exist through the exhalation of CO_2 in volcanoes on the one hand, and the subduction of calcitic and dolomitic sediments on the other. From the continental crust, a ^{87}Sr -enriched flux discharges into the oceans because the continent has a higher Rb/Sr ratio. Therefore, collisions between continents result in high $^{87}\text{Sr}/^{86}\text{Sr}$ ratios. Fragmentation, on the other hand, lowers this ratio, because more ^{86}Sr is transferred from the mantle into the crust through spreading.

Fig. 13 is intended to give a comparison of the behaviour of the kinetic mantle convection energy with the ice ages. More than 99.9 per cent of the carbon located above the Moho can be found in the crust (Garrels & MacKenzie 1972). It has arrived there for the most part via dead organisms and is withdrawn from the atmosphere. By reducing the greenhouse effect, this withdrawal leads to the ice ages; only their division into glacial episodes and interglacial episodes can be explained by the Milankovitch theory. The atmosphere is recharged with CO_2 through outgassing in volcanic regions, etc. Since one must expect an increase in the outgassing activities during episodes with a high kinetic energy of mantle convection, the ice ages should be found in the minima of E_{kin} ; Fig. 13 confirms this expectation.

Finally, we wish to compare our results with those of other authors who have studied the Earth's thermal evolution. Christensen (1984) investigated the heat transport by 2-D steady-state convection with temperature-dependent viscosity in a square box. In contrast to our paper, he assumed a given temperature contrast ΔT across the convective layer and no internal heat sources. In the first part of his paper he assumed a fixed top-to-bottom viscosity ratio and arrived at gradients $\beta = \partial \ln(Nu) / \partial \ln(Ra)$ between 0.23 and 0.36, where Ra is the Rayleigh number and Nu the Nusselt number. His conclusions of this first, more traditional part, on the Earth's evolution are similar to Schubert's (1979). In the second part of his paper, however, he assumed a fixed surface viscosity, as did we because of the previously mentioned feed-back mechanism for the surface temperature, whereas in depth there is no mechanism to keep a particular temperature or viscosity constant. Therefore, he and we arrived at very low β values. For $\beta=0$, Christensen (1984) concluded, in contrast to Schubert (1979), that the present state still depends on the initial condition, and that the Archaean lithospheric plates did not move essentially faster on average than the plates do today. Both conclusions are in concordance with our present model. The usual parameterized convection models, such as that of Schubert (1979), were based on gradients β between 0.23 and 0.36 and implicitly on Tozer's (1965, 1972) assumption of a narrow link between the average surface heat flow q_{ob} and the mean temperature of the mantle.

The first and last panels of Fig. 3 show that this assumption is not true in a fully dynamical model. With the lower value of β , Christensen (1984, 1985) computed a heat flow in the Archaean not more than 50 per cent higher than today in concordance with the first panel of our Fig. 3. Christensen (1985) also compared purely thermal evolution models with large and small β . He emphasized that very different parameterized models with $\beta \approx 0.3$ of various authors lead to the conclusion that the mantle has forgotten its initial condition, independent of the assumed Newtonian or non-Newtonian rheologies. We believe, however, that it is not a general proof, but that incorporating the flows of the different radionuclides (not only the four isotopes ^{238}U , ^{235}U , ^{232}Th and ^{40}K) also

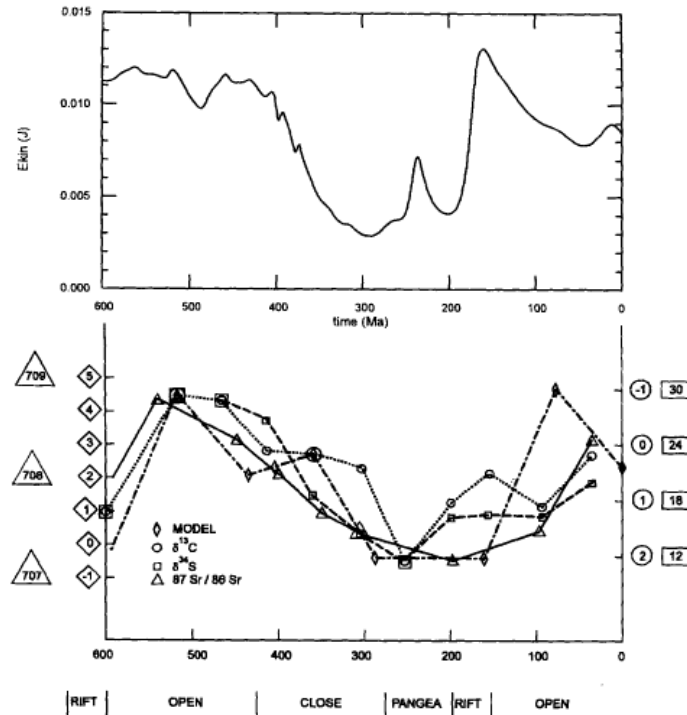


Figure 12. The E_{kin} curve of mantle convection (this work, at top) is compared here for the Phanerozoic with a diagram from Worsley *et al.* (1984) plotted against time and containing the following parameters: $\delta^{13}C$, $\delta^{34}S$, $^{87}Sr/^{86}Sr$ in deposits, and a simplified sea-level curve designated as 'model'.

other geochemical tracers) it must be feasible to draw conclusions on the starting conditions of the Earth. On the other hand, if we compare our results with Christensen's low- β models we find much of concordance, for example the surface heat transport is rather decoupled from the internal temperature; it depends more on the surface viscosity. In general, it is not easy to compare the results, because we used a two-layered non-steady model with plenty of geochemical details.

In a study of the creep deformation in olivine, Karato (1989) concluded that in the upper mantle the ratio T/T_m is between 0.5 and 0.8, the grain size is between 10 μm and 10 mm and the shear stress is between 0.1 and 100 MPa, and, therefore, using his deformation mechanism maps, both the dislocation-creep regime (non-Newtonian rheology) and the diffusion-creep regime (Newtonian rheology) are possible. For the lower mantle, Karato (1996, personal communication) prefers the Newtonian rheology. Schubert (1979) emphasized that the dependence of viscosity on temperature and pressure far outweighs any influence of a possible non-Newtonian stress-strain-rate relationship. Therefore, and for simplicity, we used a Newtonian rheology in this paper.

Papers on mantle convection are often confined to a simple partial mechanism. The behaviour of the numerical solutions of this special mechanism has been investigated by variation

of the parameters, and the physical causes of it have been discussed in detail. This procedure is legitimate. We also used the variation of parameters, e.g. Fig. 8. The results of that branch of work are, however, not considered to be derived from first principles because the mathematical form of the stress-strain-rate relationship is a hypothesis, and the magnitude of the parameters in it gives rise to controversies. Only the 10^{21} Pa s value of the shear viscosity in the asthenosphere beneath the continents seems to be unquestionable. In the lower mantle, there must be regions with elevated viscosity, but the details of modern models differ considerably. The modelling of slab penetration in a homogeneous 10^{21} Pa s mantle by Ricard, Spada & Sabadini (1993) reveals a very unstable rotational axis. For the lower mantle, a viscosity of at least 10^{22} Pa s is necessary to reduce the computed rate of true polar wander to palaeomagnetically observed values.

In contrast to these uncertainties, the existence of continents and oceans over nearly the entire time span of the Earth's evolution, the existence of geochemical reservoirs and the magnitude of the abundances of ^{238}U , ^{235}U , ^{232}Th and ^{40}K in them are better known. Therefore, we wish to emphasize that we believe that our approach is suitable for an Earth evolution model, although the mentioned uncertainties of the other models could not be excluded.

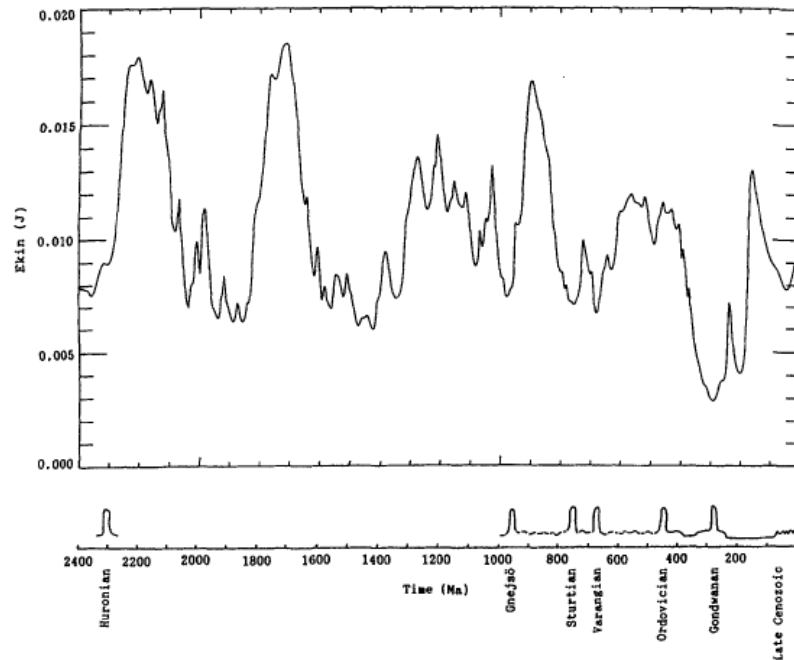


Figure 13. Top: the kinetic energy of mantle convection (this work); bottom, the ice ages are plotted over the geological age (Tarling 1978; Crowley 1983).

4 CONCLUDING REMARKS

The principal aim of this paper was to study the influence of a simplified chemical segregation in the mantle, which leads to the formation of the continental crust, on the time dependence of the thermal convection in the mantle. Our study is based on a realistic distribution of the abundances of the major heat-producing isotopes. This distribution has changed through thermal mantle convection with chemical segregation in the course of the Earth's history and has led to the size of the present continents, a depleted upper mantle, realistic distributions of the viscosity, temperature and flow velocity and to a correct recent heat flow on the surface of the Earth. The activation enthalpy of the strongly temperature-dependent viscosity has been estimated with the help of the following melting curves: for the upper mantle, that of Ito & Takahashi (1987), for the upper part of the lower mantle, that of Heinz & Jeanloz (1987), and for the middle and lower parts of the lower mantle, that of Knittle & Jeanloz (1989). The last two are intended to apply to perovskite. We have planned studies involving other melting-point curves and other methods for estimating the activation enthalpy for the future. The choice of the initial conditions was influenced by considerations concerning the cosmogony of the Earth and by the geochemical investigations outlined in Section 2.4.

The internal radiogenic heating, a strongly non-linear dependence of the shear viscosity on temperature and a simple

chemical segregation mechanism are the essentials of our model. It results in time variations of the convective intensity. For an acceptable choice of parameters we received an approximate correlation of these variations with the distribution of mineral date abundances or magmatic activity. The viscosity has a relative maximum at a depth of 670 km. In the greater part of the lower mantle, the viscosity rises strongly with increasing depth. The lowermost part of the lower mantle is sluggish. The lowermost mantle forms a reference frame for plumes. The lack of change of location of plumes could be connected with this feature of the model.

ACKNOWLEDGMENTS

We thank Harro Schmeling for kindly transferring his code for the calculation of 2-D thermal convection. We used it as a starting variant for the development of our code. Furthermore, we gratefully acknowledge his and an anonymous reviewer's helpful discussions and comments on the manuscript.

REFERENCES

- Abbott, D. & Mooney, W., 1995. The crustal and geochemical evolution of the continental crust: Support for the oceanic plateau model of continental growth. *Rev. Geophys., Suppl.*, US National Report to IUGG, Paper no. 95RG00551, 231-242.

- Agee, C.B., 1990. Melting of Allende at 26 GPa: a new look at mantle differentiation and core formation, *Nature*, **346**, 834–837.
- Akaogi, M. & Ito, E., 1993. Refinement of enthalpy measurement of MgSiO_3 perovskite and negative pressure–temperature slopes for perovskite-forming reactions, *Geophys. Res. Lett.*, **20**, 1839–1842.
- Allègre, C.J. & Lewin, E., 1989. Chemical structure and history of the Earth: evidence from global non-linear inversion of isotopic data in a three-box model, *Earth planet. Sci. Lett.*, **96**, 61–88.
- Anders, E. & Grevesse, N., 1989. Abundances of elements: Meteoritic and solar, *Geochim. Cosmochim. Acta*, **53**, 197–214.
- Arculus, R.J., Holmes, R.D., Powell, R. & Righter, K., 1990. Metal-silicate equilibria and core formation, in *Origin of the Earth*, pp. 251–271, eds Newsom, H.E. & Jones, J.H., Oxford University Press, New York, NY.
- Armstrong, R.L., 1981. Radiogenic isotopes: the case for crustal recycling on a near-steady-state no-continental-growth Earth, *Phil. Trans. R. Soc. Lond. A*, **301**, 443–472.
- Benz, W. & Cameron, A.G.W., 1990. Terrestrial effects of the giant impact, in *Origin of the Earth*, pp. 61–67, eds Newsom, H.E. & Jones, J.H., Oxford University Press, New York, NY.
- Bickle, M.J., 1978. Heat loss from the Earth: A constraint on Archaean tectonics from the relation between geothermal gradients and the rate of plate production, *Earth planet. Sci. Lett.*, **40**, 301–315.
- Biéumont, E., Baudoux, M., Kurucz, R.L., Ansbacher, W. & Pinnington, E. H., 1991. The solar abundance of iron: A 'final' word! *Astron. Astrophys.*, **249**, 539–544.
- Billington, S., 1978. The morphology and tectonics of subducted lithosphere in the Tonga–Fiji–Kermadec region from seismicity and focal mechanism solutions, *PhD thesis*, Cornell University, Ithaca, NY.
- Boss, A.P., 1990. 3-D solar nebula models: Implications for Earth origin, in *Origin of the Earth*, pp. 3–15, eds Newsom, H.E. & Jones, J.H., Oxford University Press, New York, NY.
- Boussinesq, J., 1903. *Théorie Analytique de la Chaleur mise en Harmonie avec la Thermodynamique et avec la Théorie Mécanique de la Lumière*, Tome II, pp. 157–176, Gauthier-Villars, Paris.
- Bunge, H.P., Richards, M.A. & Baumgardner, J.R., 1996. A sensitivity study of 3-D spherical mantle convection at 10^8 Rayleigh number: Effects of depth-dependent viscosity, heating mode and an endothermic phase change, submitted.
- Burke, K. & Kidd, W.S.F., 1978. Were Archaean continental geothermal gradients much steeper than those of today?, *Nature*, **727**, 240–241.
- Burke, W.H., Denison, R.E., Hetherington, E.A., Koepnick, R.B., Nelson, H.F. & Otto, J.B., 1982. Variation of seawater $^{87}\text{Sr}/^{86}\text{Sr}$ throughout Phanerozoic time, *Geology*, **10**, 516–519.
- Cameron, A.G.W., 1978. Physics of the primitive solar accretion disk, *Moon Planets*, **18**, 5–40.
- Cameron, A.G.W., 1988. Origin of the solar system, *Ann. Rev. Astron. Astrophys.*, **26**, 441–472.
- Cameron, A.G.W. & Ward, W.R., 1976. The origin of the Moon, *Lunar Sci.*, **7**, 120–130.
- Campbell, I.H. & Griffiths, R.W., 1992. The changing nature of mantle hotspots through time: Implications of the chemical evolution of the mantle, *J. Geol.*, **92**, 497–523.
- Christensen, U.R., 1984. Heat transport by variable viscosity convection and implications for the Earth's thermal evolution, *Phys. Earth planet. Inter.*, **35**, 264–282.
- Christensen, U.R., 1985. Thermal evolution models for the Earth, *J. geophys. Res.*, **90**, 2995–3007.
- Christensen, U.R. & Hofmann, A.W., 1994. Segregation of subducted oceanic crust in the convecting mantle, *J. geophys. Res.*, **99**, 19867–19884.
- Christensen, U.R. & Yuen, D.A., 1989. Time-dependent convection with non-Newtonian viscosity, *J. geophys. Res.*, **94**, 814–820.
- Claypool, G.E., Holsler, W.T., Kaplan, I.R., Sakai, H. & Zak, I., 1980. The age curves of sulfur and oxygen isotopes in marine sulfate and their mutual interpretation, *Chem. Geol.*, **28**, 199–259.
- Coffin, M.F. & Eldholm, O., 1994. Large igneous provinces: Crustal structure, dimensions, and external consequences, *Rev. Geophys.*, **32**, 1–36.
- Crowley, T.J., 1983. The geologic record of climatic change, *Rev. Geophys. Space Phys.*, **21**, 828–877.
- Dasch, E.J., Ryder, G. & Nyquist, L.E., 1988. Chronology and complexity of early lunar crust, *Tectonophysics*, **161**, 157–164.
- DePaolo, D.J., 1988. *Neodymium Isotope Geochemistry*, Springer-Verlag, Berlin.
- Dickinson, W.R. & Luth, W.C., 1971. A model for plate tectonic evolution of mantle layers, *Science*, **174**, 400–404.
- Gaffey, M.J., 1990. Thermal history of the asteroid belt: Implications for accretion of the terrestrial planets, in *Origin of the Earth*, pp. 17–28, eds Newsom, H.E. & Jones, J.H., Oxford University Press, New York, NY.
- Galer, S.J.G., Goldstein, S.I. & O'Nions, R.K., 1989. Limits on chemical and convective isolation in the Earth's interior, *Chem. Geol.*, **75**, 257–290.
- Garrels, R.M. & MacKenzie, F.T., 1972. A quantitative model for the sedimentary rock cycle, *Mar. Chem.*, **1**, 27–41.
- Gastil, G., 1960. The distribution of mineral dates in time and space, *Am. J. Sci.*, **258**, 1–35.
- Giardini, D. & Woodhouse, J.H., 1984. Deep seismicity and modes of deformation in Tonga subduction zone, *Nature*, **307**, 505–509.
- Graham, D.W., Zhou, H.-W., Yuen, D.A. & Reuteler, D.M., 1996. Tomographic evidence for the transition zone as a high $^3\text{He}/^4\text{He}$ reservoir, University of Minnesota Supercomputer Institute Research Report UMSI 96/11, *Earth planet. Sci. Lett.*, submitted.
- Hansen, U. & Ebel, A., 1988. Time dependent thermal convection—a possible explanation for a multiscale flow in the Earth's mantle, *Geophys. J.*, **94**, 181–191.
- Hart, S.R., 1988. Heterogeneous mantle domains: signatures and mixing chronologies, *Earth planet. Sci. Lett.*, **90**, 273–296.
- Hart, S. & Zindler, A., 1989. Constraints on the nature and development of chemical heterogeneities in the mantle, in *Mantle Convection, Plate Tectonics and Global Dynamics*, pp. 261–387, ed. Peltier, W.R., Gordon & Breach, New York, NY.
- Heinz, D.L. & Jeanloz, R., 1987. Measurement of the melting curve of $\text{Mg}_{0.9}\text{Fe}_{0.1}\text{SiO}_3$ at lower mantle conditions and its geophysical implications, *J. geophys. Res.*, **92**, 11437–11444.
- Hofmann, A.W., 1988. Chemical differentiation of the Earth: the relationship between mantle, continental crust, and oceanic crust, *Earth planet. Sci. Lett.*, **90**, 297–314.
- Holweger, H., Heise, C. & Kock, M., 1990. The abundance of iron in the Sun derived from the photospheric Fe II lines, *Astron. Astrophys.*, **232**, 510–515.
- Honda, S., Balachandrar, S., Yuen, D.A. & Reuteler, D., 1993. Three-dimensional instabilities of mantle convection with multiple phase transitions, *Science*, **259**, 1308–1311.
- Ida, S. & Makino, J., 1993. Scattering of planetesimals by a protoplanet: Slowing down of runaway growth, *Icarus*, **106**, 210–227.
- Isacks, B. & Molnar, P., 1969. Mantle earthquake mechanisms and sinking of the lithosphere, *Nature*, **223**, 1121–1124.
- Ita, J. & King, S.D., 1994. Sensitivity of convection with an endothermic phase change to the form of governing equations, initial conditions, boundary conditions, and equation of state, *J. geophys. Res.*, **99**, 15919–15938.
- Ito, E. & Takahashi, E., 1987. Melting of peridotite at uppermost lower-mantle conditions, *Nature*, **328**, 514–517.
- Jacobsen, S.B., 1988. Isotopic and chemical constraints on mantle-crust evolution, *Geochim. Cosmochim. Acta*, **52**, 1341–1350.
- Jacobsen, S.B. & Wasserburg, G.J., 1979. The mean age of mantle and crustal reservoirs, *J. geophys. Res.*, **84**, 7411–7427.
- Jagoutz, E. et al. 1979. The abundances of major, minor, and trace elements in the Earth's mantle as derived from primitive ultramafic nodules, *Proc. Lunar Planet. Sci. 10th Conf.*, 2031–2050.
- Jarvis, G.T. & Peltier, W.R., 1989. Convection models and geophysical observations, in *Mantle Convection, Plate Tectonics and Global*

- Dynamics*, pp. 479–593, ed. Peltier, W.R., Gordon & Breach, New York, NY.
- Jochum, K.P., Hofmann, A.W., Seufert, M. & White, W.M., 1988. The composition of mid-ocean ridge basalt, manuscript.
- Karato, S.-I., 1989. Defects and plastic deformation in olivine, in *Rheology of Solids and of the Earth*, pp. 176–208, eds Karato, S.-I. & Toriumi, M., Oxford University Press, Oxford.
- Kargel, J.S. & Lewis, J.S., 1993. The composition and early evolution of Earth, *Icarus* **105**, 1–25.
- Kerridge, J.F., 1993. What can meteorites tell us about nebular conditions and processes during planetesimal accretion?, *Icarus* **106**, 135–150.
- Knittle, E. & Jeanloz, R., 1989. Melting curve of (Mg,Fe)SiO₃ perovskite to 96 GPa: evidence for a structural transition in lower mantle melts, *Geophys. Res. Lett.*, **16**, 421–424.
- Kohlstedt, D.L. & Goetze, C., 1974. Low stress high temperature creep of olivine single crystals, *J. geophys. Res.*, **85**, 3122–3130.
- Kröner, A., 1985. Evolution of the Archaean continental crust, *Ann. Rev. Earth planet. Sci.*, **13**, 49–74.
- Leitch, A.M. & Yuen, D.A., 1989. Internal heating and thermal constraints on the mantle, *Geophys. Res. Lett.*, **16**, 1407–1410.
- Machetel, P. & Yuen, D.A., 1989. Penetrative convective flows induced by internal heating and mantle compressibility, *J. geophys. Res.*, **94**, 10609–10626.
- McKenzie, D. & Bickle, M.H., 1988. The volume and composition of melt generated by extension of the lithosphere, *J. Petrol.*, **29**, 625–679.
- McKenzie, D.P. & Weiss, N.O., 1975. *Geophys. J. R. astr. Soc.*, **42**, 131.
- Meissner, R., 1986. *The Continental Crust, a Geophysical Approach*, Academic Press, Orlando, FL.
- Melosh, H.J., 1990. Giant impacts and the thermal state of the early Earth, in *Origin of the Earth*, pp.69–83, eds Newsom, H.E. & Jones, J.H., Oxford University Press, New York, NY.
- Mizuno, H., 1980. Formation of the giant planets, *Prog. Theor. Phys.*, **64**, 544–557.
- Mizuno, H. & Nakazawa, K., 1988. Primordial atmosphere surrounding a protoplanet and formation of jovian planets, *Prog. Theor. Phys. Suppl.*, **95**, 266–273.
- Nataf, H.C. & Richter, F.M., 1982. Convection experiments in fluids with highly temperature dependent viscosity and the thermal evolution of the Earth, *Phys. Earth planet. Inter.*, **29**, 320–329.
- Newsom, H.E. & Taylor, S.R., 1989. Geochemical implications of the formation of the Moon by a single giant impact, *Nature*, **338**, 29–34.
- Oberbeck, A., 1879. Über die Wärmeleitung der Flüssigkeiten bei Berücksichtigung der Strömungen infolge von Temperaturdifferenzen, *Ann. Physik Chemie, Neue Folge*, **7**, 271–292.
- Oberbeck, A., 1880. Strömungen von Flüssigkeiten infolge ungleicher Temperaturen innerhalb derselben, *Ann. Phys. Chem., Neue Folge*, **11**, 489–495.
- O'Nions, R.K., Evensen, N.M. & Hamilton, P.J., 1979. Geochemical modeling of mantle differentiation and crustal growth, *J. geophys. Res.*, **84**, 6091–6101.
- Ogawa, M., 1993. A numerical model of a coupled magmatism–mantle convection system in Venus and the Earth's mantle beneath Archaean continental crusts, *Icarus*, **102**, 40–61.
- Peltier, W.R. & Solheim, L.P., 1992. Mantle phase transitions, layered chaotic convection, and the viscosity of the deep mantle, in *Chaotic Processes in the Geological Sciences*, pp. 111–139, ed. Yuen, A., Springer-Verlag, New York, NY.
- Pollack, H.N., Hurter, S.J. & Johnson, J.R., 1993. Heat flow from the Earth's interior: Analysis of the global data set, *Rev. Geophys.*, **31**, 267–280.
- Quarení, F. & Yuen, D.A., 1988. Mean-field methods in mantle convection, in *Mathematical Geophysics*, pp. 227–264, eds Vlaar, N.J., Nolet, G., Wortel, M.J.R. & Cloeting, S.A.P.L., D. Reidel, Dordrecht.
- Quarení, F. & Mulargia, F., 1989. The Grüneisen parameter and adiabatic gradient in the Earth's interior, *Phys. Earth planet. Inter.*, **55**, 221–233.
- Rampino, M.R. & Caldeira, K., 1993. Major episodes of geologic change: correlations, time structure and possible causes, *Earth planet. Sci. Lett.*, **114**, 215–227.
- Ranalli, G., 1991. The microphysical approach to mantle rheology, in *Glacial Isostasy, Sea Level and Mantle Rheology*, pp. 343–378, eds Sabadini, R., Lambeck, K. & Boschi, E., Kluwer Academic, Dordrecht.
- Reymer, A. & Schubert, G., 1984. Phanerozoic addition rates to the continental crust and crustal growth, *Tectonics*, **3**, 63–77.
- Ricard, Y., Spada, G. & Sabadini, R., 1993. Polar wandering of a dynamic earth, *Geophys. J. Int.*, **113**, 284–298.
- Ringwood, A.E., 1975. *Composition and Petrology of the Earth's Mantle*, McGraw-Hill, New York, NY.
- Ringwood, A. E., 1982. Phase transformations and differentiation in subducted lithosphere: Implications for mantle dynamics, basalt petrogenesis, and crustal evolution, *J. Geol.*, **90**, 611–643.
- Ringwood, A.E., 1990. Earliest history of the Earth-Moon system, in *Origin of the Earth*, pp. 101–134, eds Newsom, H.E. & Jones, J.H., Oxford University Press, New York, NY.
- Safronov, V.S., 1962. Velocity dispersion in rotating systems of gravitating bodies with inelastic collisions (in Russian), *Voprosy Kosmogonii*, **8**, 168–179.
- Safronov, V.S., 1969. Evolution of the protoplanetary cloud and formation of the Earth and planets, Nauka, Moscow. [Transl. 1972 NASA TT F-677.]
- Safronov, V.S., 1991. Kuiper prize lecture: Some problems in the formation of the planets, *Icarus*, **94**, 260–271.
- Schmeling, H. & Bussod, G.Y., 1996. Variable viscosity convection and partial melting in the continental asthenosphere, *J. geophys. Res.*, **101**, 5411–5423.
- Schmeling, H. & Marquart, G., 1993. Mantle flow and the evolution of the lithosphere, *Phys. Earth planet. Inter.*, **79**, 241–267.
- Schmidt, O.J., 1957. *Four lectures on the theory of the origin of the Earth* (in Russian), Izd. 3, dop. M., Izd-vo AN SSSR.
- Schubert, G., 1979. Subsidiary convection in the mantles of terrestrial planets, *Ann. Rev. Earth planet. Sci.*, **7**, 289–342.
- Schubert, G. & Young, R. E., 1976. Cooling the Earth by whole mantle subsolidus convection: A constraint on the viscosity of the lower mantle, *Tectonophysics*, **35**, 201–214.
- Schubert, G., Cassen, P. & Young, R. E., 1979. Subsidiary convective cooling histories of the terrestrial planets, *Icarus*, **38**, 192–211.
- Şengör, A.M.C., 1990. Plate tectonics and orogenic research after 25 years: a Tethyan perspective, *Earth Science Rev.*, **27**, 1–201.
- Spada, G., Sabadini, R. & Yuen, D.A., 1991. The dynamical influences of a hard transition zone on post-glacial uplifts and rotational signatures, in *Glacial Isostasy, Sea-Level and Mantle Rheology*, pp. 121–141, eds Sabadini, R., Lambeck, K. & Boschi, E., Kluwer Academic, Dordrecht.
- Spohn, T. & Breuer, D., 1993. Mantle differentiation through continental crust growth and recycling and the thermal evolution of the Earth, in *Evolution of the Earth and Planets*, pp. 55–71, eds Takahashi, E., Jeanloz, R. & Rubie, D., Geophysical Monograph 74, IUGG Volume 14, AGU.
- Stevenson, D.J., 1990. Fluid dynamics of core formation, in *Origin of the Earth*, pp. 231–249, eds Newsom, H.E. & Jones, J.H., Oxford University Press, New York, NY.
- Stille, H., 1944. Geotektonische Gliederung der Erdgeschichte, *Abh. Preuss. Akad. Wiss., Math. Naturwiss. Kl.*, **3**, 1–80.
- Tackley, P.J., Stevenson, D.J., Glatzmaier, G.A. & Schubert, G., 1993. Effects of an endothermic phase transition at 670 km depth in a spherical model of convection in the Earth's mantle, *Nature*, **361**, 699–704.
- Tarling, D.H., 1978. The geological–geophysical framework of ice ages, in *Climatic Change*, pp. 3–24, ed Gribbin, J., Cambridge University Press, New York, NY.

- Taylor, S.R., 1992. *Solar System Evolution. A New Perspective*. Cambridge University Press, Cambridge.
- Taylor, S.R. & Norman, M.D., 1990. Accretion of differentiated planetesimals to the Earth, in *Origin of the Earth*, pp.29–43, eds Newsom, H.E. & Jones, J.H., Oxford University Press, Oxford.
- Titley, S.R., 1993. Relationship of stratabound ores with tectonic cycles of the Phanerozoic and Proterozoic, *Precambrian Res.*, **61**, 295–322.
- Tozer, D.C., 1965. Heat transfer and convection currents, *Phil. Trans. R. Soc. Lond. A*, **258**, 252–271.
- Tozer, D.C., 1972. The present thermal state of the terrestrial planets, *Phys. Earth planet. Inter.*, **6**, 182–197.
- Van Schmus, W.R., 1989. Radioactivity properties of minerals and rocks, in *Practical Handbook of Physical Properties of Rocks and Minerals*, pp.583–596, ed Carmichael, R. S., CRC Press, Boca Raton, Ann Arbor, Boston, MA.
- Weizer, J., Holser, W.T. & Wilgus, C.K., 1980. Correlation of $^{13}\text{C}/^{12}\text{C}$ and $^{34}\text{S}/^{32}\text{S}$ secular variations, *Geochim. Cosmochim. Acta*, **44**, 579–587.
- Weizer, J., Compston, W., Clauer, N. & Schidlowski, M., 1983. $^{87}\text{Sr}/^{86}\text{Sr}$ in late Proterozoic carbonates: Evidence for a 'mantle' event at 900 Myr ago, *Geochim. Cosmochim. Acta*, **47**, 295–302.
- Walzer, U., 1981. Untersuchung der Konvektion im Erdinneren und dafür wichtiger Materialparameter unter hohem Druck, *Veröff. Zentralinst. Physik d. Erde*, **75**, 1–256.
- Wänke, H., Dreibus, G. & Jagoutz, E., 1984. Mantle chemistry and accretion history of the Earth, in *Archaean Geochemistry*, pp.1–24, eds Kröner, A., Hanson, G.N. & Goodwind, A.M., Springer-Verlag, Berlin.
- Warren, P.H., 1989. Growth of the continental crust: A planetary mantle perspective, *Tectonophysics*, **161**, 165–199.
- Weinstein, S.A., Olson, P.L. & Yuen, D.A., 1989. Time-dependent large aspect-ratio thermal convection in the Earth's mantle, *Geophys. Astrophys. Fluid Dyn.*, **47**, 157–197.
- Wells, P.R.A., 1976. Late Archaean metamorphism in the Buksef jorden region, S. W. Greenland, *Contrib. Mineral. Petrol.*, **56**, 229–242.
- Wetherill, G.W., 1990. Formation of the Earth, *Ann. Rev. Earth planet. Sci.*, **18**, 205–256.
- Wetherill, G.W. & Stewart, G.R., 1993. Formation of planetary embryos: Effects of fragmentation, low relative velocity, and independent variation of eccentricity and inclination, *Icarus*, **106**, 190–209.
- Windley, B.F., 1984. *The Evolving Continents*, 2nd edn. Wiley, New York, NY.
- Worsley, T.R., Nance, D. & Moody, J.B., 1984. Global tectonics and eustasy for the past 2 billion years, *Mar. Geol.*, **58**, 373–400.
- Wuchterl, G., 1989. Zur Entstehung der Gasplaneten. Kugelsymmetrische Gasströmungen auf Protoplaneten, *Diss. Univ. Wien, Institut für Astronomie*, 1–156.
- Zhao, W., Yuen, D.A. & Honda, S., 1992. Multiple phase transitions and the style of mantle convection, *Phys. Earth planet. Inter.*, **72**, 185–210.

APPENDIX A: BASIC EQUATIONS

The full set of equations describing thermal convection in the Earth's mantle consists of the conservation equation of mass:

$$\frac{d\rho}{dt} + \rho \frac{\partial v_i}{\partial x_i} = 0; \quad (\text{A1})$$

of momentum:

$$\rho \frac{dv_k}{dt} = \rho b_k + \frac{\partial \sigma_{ik}}{\partial x_i}, \quad (\text{A2})$$

and of energy:

$$\rho \frac{du}{dt} + \frac{\partial q_i}{\partial x_i} = Q + \sigma_{ik} \dot{\epsilon}_{ik}. \quad (\text{A3})$$

The conservation of angular momentum yields

$$\sigma_{ik} = \sigma_{ki}. \quad (\text{A4})$$

Stress tensor σ_{ik} and strain-rate tensor $\dot{\epsilon}_{ik}$ are related by the Navier–Poisson law of a viscous fluid:

$$\sigma_{ik} = -p\delta_{ik} + \lambda\dot{\epsilon}_{ij}\delta_{ik} + 2\eta\dot{\epsilon}_{ik}, \quad (\text{A5})$$

while the strain rate is connected with the velocity v_i by

$$\dot{\epsilon}_{ik} = \frac{1}{2} \left(\frac{\partial v_i}{\partial x_k} + \frac{\partial v_k}{\partial x_i} \right). \quad (\text{A6})$$

The kinetic equation of state relates pressure p , density ρ and temperature T :

$$F(p, \rho, T) = 0, \quad (\text{A7})$$

while the caloric equation of state gives the specific internal energy u :

$$u = u(T, \rho). \quad (\text{A8})$$

Finally the conductive heat flow q_k is given by Fourier's law of heat conduction:

$$q_k = -k \frac{\partial T}{\partial x_k}. \quad (\text{A9})$$

Eqs (A1) to (A9) result in 25 equations of 25 variables, summarized in Table A1. The number of variables of the stress tensor σ_{ik} has been taken as nine because eq. (A4) is included.

The time t and the location vector \mathbf{r} are the independent variables. The gravity acceleration b_k , heat conductivity k and volume viscosity λ are given quantities. The heat production rate per volume Q is assigned to individual particles (tracers) that are carried along with the flow. Q is time-dependent, according to the law of radioactive decay. At thermodynamically defined locations, chemical differentiation takes place, leading to geochemically acceptable present source distributions, as will be described in greater detail in the text. The shear viscosity η is a function of temperature. For the substantial time derivative the following abbreviation is used:

$$\frac{d}{dt} \dots = \frac{\partial}{\partial t} \dots + \mathbf{v} \cdot \nabla \dots \quad (\text{A10})$$

Using the first law of thermodynamics, the specific internal energy has been eliminated. As a linearized kinetic equation of state, we select

$$\rho = \rho_0 [1 - \alpha(T - T_0)]. \quad (\text{A11})$$

We use a 2-D flow model of an Oberbeck–Boussinesq fluid at infinite Prandtl number Pr . This means that the density is

Table A1. Variables of the problem.

Number of variables	Symbol	Description of the variable
3	v_k	Velocity components
1	T	(Absolute) temperature
1	u	Specific internal energy
1	ρ	Density
9	σ_{ik}	Stress-tensor components
6	$\dot{\epsilon}_{ik}$	Strain-rate tensor components
3	q_k	Heat-flux components
1	p	Thermodynamic pressure

assumed constant except for thermally induced variations in the buoyancy term, and that inertial forces may be neglected. Moreover, it follows that the flow is incompressible, i.e. $\nabla \cdot \mathbf{v} = 0$. Consequently, we can represent the horizontal component u and the vertical component w of the velocity by the scalar stream function ψ :

$$u = \frac{\partial \psi}{\partial z} \quad \text{and} \quad w = -\frac{\partial \psi}{\partial x}. \quad (\text{A12})$$

Also, the Oberbeck–Boussinesq approximation implies the neglect of adiabatic and viscous heating.

The heat-flux vector, the specific heat production and the heat produced per unit time per unit volume are designated by q (W m^{-2}), H (W kg^{-1}) and Q (W m^{-3}) respectively. Using the following scaling scheme, non-dimensional variables are introduced. The index ‘0’ relates to the surface of the model. The primed quantities relate here to non-dimensional variables. They will be dropped elsewhere.

$$\rho = \rho_0 \rho'; \quad x = hx'; \quad z = hz'; \quad \mathbf{v} = \frac{\kappa}{h} \mathbf{v}'; \quad t = \frac{h^2}{\kappa} t';$$

$$p = \frac{\kappa \eta_0}{h^2} p' - \rho_0 g h z'; \quad \tau_{ij} = \frac{\kappa \eta_0}{h^2} \tau'_{ij}; \quad \eta = \eta_0 \eta';$$

$$T = \Delta T_0 T' + T_0; \quad \psi = \psi' \kappa;$$

$$H = \frac{c_p \Delta T_0 \kappa}{h^2} H';$$

$$q = \frac{c_p \Delta T_0 \kappa \rho_0}{h} q'; \quad \text{magnitude of the heat flux}$$

$$A = \eta_0^n \left(\frac{\kappa}{h^2} \right)^{n-1} A'; \quad E_0 = \Delta T_0 R E'_0;$$

$$V_0 = \frac{R \Delta T_0}{\rho_0 g h} V'_0; \quad T_m = \Delta T_0 T'_m + T_0.$$

ρ_0 is the density at reference temperature T_0 , h is the depth of the convecting layer, t is the time, κ is the thermal diffusivity, η_0 is a reference shear viscosity, τ_{ij} is the deviatoric stress, ΔT_0 is a reference temperature contrast, c_p is the specific heat at constant pressure, R is the gas constant, E_0 is the activation energy and V_0 is the activation volume.